

# Systems Approaches to Unravel Molecular Function: High-content siRNA Screen Identifies TMEM16A Traffic Regulators as Potential Drug Targets for Cystic Fibrosis

Madalena C. Pinto<sup>1</sup>, Hugo M. Botelho<sup>1</sup>, Iris A. L. Silva<sup>1</sup>, Violeta Railean<sup>1</sup>, Beate Neumann<sup>2</sup>, Rainer Pepperkok<sup>2</sup>, Rainer Schreiber<sup>3</sup>, Karl Kunzelmann<sup>3</sup> and Margarida D. Amaral<sup>1\*</sup>

**1 - BioISI - Biosystems & Integrative Sciences Institute, Faculty of Sciences, University of Lisboa, Campo Grande, C8, 1749-016 Lisboa, Portugal**

**2 - Cell Biology/Biophysics Unit, and ALMF, European Molecular Biology Laboratory (EMBL), 69117 Heidelberg, Germany**

**3 - Institut für Physiologie, University of Regensburg, Universitätsstraße 31, D-93053 Regensburg, Germany**

**Correspondence to Margarida D. Amaral:** [mdamaral@fc.ul.pt](mailto:mdamaral@fc.ul.pt) (M.D. Amaral), [@madalenacpinto](https://twitter.com/madalenacpinto) (M.C. Pinto)  
<https://doi.org/10.1016/j.jmb.2021.167436>

**Edited by Igor Stagljar**

## Abstract

An attractive approach to treat people with Cystic Fibrosis (CF), a life-shortening disease caused by mutant CFTR, is to compensate for the absence of this chloride/bicarbonate channel by activating alternative (non-CFTR) chloride channels. One obvious target for such “mutation-agnostic” therapeutic approach is TMEM16A (anoctamin-1/ANO1), a calcium-activated chloride channel (CaCC) which is also expressed in the airways of people with CF, albeit at low levels. To find novel TMEM16A regulators of both traffic and function, with the main goal of identifying candidate CF drug targets, we performed a fluorescence cell-based high-throughput siRNA microscopy screen for TMEM16A trafficking using a double-tagged construct expressed in human airway cells. About 700 genes were screened (2 siRNAs per gene) of which 262 were identified as candidate TMEM16A modulators (179 siRNAs enhanced and 83 decreased TMEM16A traffic), being G-protein coupled receptors (GPCRs) enriched on the primary hit list. Among the 179 TMEM16A traffic enhancer siRNAs subjected to secondary screening 20 were functionally validated. Further hit validation revealed that siRNAs targeting two GPCRs – ADRA2C and CXCR3 – increased TMEM16A-mediated chloride secretion in human airway cells, while their overexpression strongly diminished calcium-activated chloride currents in the same cell model. The knockdown, and likely also the inhibition, of these two TMEM16A modulators is therefore an attractive potential therapeutic strategy to increase chloride secretion in CF.

© 2022 Elsevier Ltd. All rights reserved.

## Introduction

Cystic Fibrosis (CF) is a life-threatening autosomal recessive disease caused by mutations in the CFTR (CF Transmembrane Conductance Regulator) gene,<sup>1,2</sup> which encodes a cAMP-regulated chloride (Cl<sup>-</sup>) and bicarbonate (HCO<sub>3</sub><sup>-</sup>) channel expressed at the apical membrane of epithelial cells.<sup>3</sup> CFTR dysfunction destabilizes the

epithelial ion and water homeostasis, and possibly also pH, resulting in dehydrated lung secretions, enhanced mucus viscosity and impaired mucociliary clearance (MCC), culminating in progressive obstruction of the airways.<sup>4,5</sup>

More than 2,100 CFTR genetic variants have been reported, of which ~360 are confirmed as CF-causing mutations. Various CFTR modulators have been approved for clinical use for individuals

with specific CF genotypes. Recently, a new highly effective CFTR modulator therapy, consisting of a combination of two correctors and one potentiator (Trikafta/Kaftrio<sup>®</sup>) was approved for people over 12 years old carrying at least one copy of the most common CFTR mutation, F508del, which represents around 80% of all people with CF worldwide.<sup>6,7</sup> Although these drugs are significantly improving the quality of life of individuals carrying this mutation, they cannot be used to pharmacologically rescue all CFTR mutations, e.g., large gene deletions or frameshift mutations. Hence, people with CF bearing these non-rescuable mutations<sup>8</sup> (also grouped as Class VII), and other mutations which are not eligible for Trikafta, still lack an effective therapy and constitute ~20%.<sup>9</sup> Although gene therapy/editing constitutes an appealing approach,<sup>10</sup> efficacious and safe protocols are still not foreseen in the short/medium term.

An interesting alternative is to develop “mutation-agnostic” therapies, namely through the activation of other (non-CFTR) anion channels that could compensate for the absence of CFTR-mediated  $\text{Cl}^-/\text{HCO}_3^-$  secretion. Anoctamin 1 (ANO1)/TMEM16A, a calcium ( $\text{Ca}^{2+}$ )-activated  $\text{Cl}^-$  channel (CaCC)<sup>11–13</sup> expressed in lung epithelia,<sup>14</sup> is one of the most promising alternative channels that can compensate for the absence of epithelial CFTR-mediated anion secretion in CF.<sup>15–17</sup>

TMEM16A has a fundamental importance for  $\text{Ca}^{2+}$ -dependent  $\text{Cl}^-$  secretion in numerous tissues, namely in the airways, salivary gland, pancreatic gland, and hepatocytes.<sup>18–20</sup> There is, however, some controversy in the field since some authors question whether activation of TMEM16A will have a positive impact in the lives of people with CF, mostly because TMEM16A has been claimed to play a positive role in mucus secretion, this implying that its activation may possibly cause further harm for people with respiratory obstructive diseases. TMEM16A has been associated with goblet cell metaplasia, as its expression is strongly upregulated concomitantly with mucus hypersecretion.<sup>21,22</sup> Additionally, during inflammation, TMEM16A expression is increased namely by Th2 interleukins (IL-4 and IL-13), particularly in mucus producing cells, with only little expression in ciliated cells.<sup>23</sup> A number of studies has shown that inhibition of TMEM16A occurs alongside with decreased mucus secretion in primary human airway surface epithelial cells<sup>24</sup> and also in intestinal cells,<sup>22</sup> thus proposing a causal relationship between the two events. Notwithstanding, other studies indicate that there is no causal link between TMEM16A and production of MUC5AC, the main constituent of human respiratory mucus and that cell proliferation is the main driver of TMEM16A upregulation.<sup>25</sup> Indeed, it was demonstrated that in the absence of proliferation (goblet cell metaplasia) MUC5AC is still upregulated, but not TMEM16A. Moreover, the same studies indicate that TMEM16A inhibition has a neg-

ative impact in airways homeostasis by decreasing the height of airway surface liquid, thus causing airway dehydration.<sup>25</sup> Additionally, it has been recently shown that a TMEM16A potentiator (ETX001, Enterprise Therapeutics) increases anion secretion and ASL height in primary human bronchial epithelial cells from individuals with CF, and promotes MCC in in vivo sheep models,<sup>26</sup> without any stimulation of airway mucus secretion.<sup>27</sup> Another important aspect to consider is the relationship between TMEM16A and CFTR, since tissue-specific TMEM16A-KO in mouse intestine and airways not only eliminates  $\text{Ca}^{2+}$ -activated  $\text{Cl}^-$  currents, but also abrogates CFTR-mediated  $\text{Cl}^-$  secretion, similarly to human cells.<sup>28</sup> Thus, we propose that potentiating TMEM16A trafficking and, consequently, its function as a  $\text{Cl}^-$  channel, is a potentially good approach to take advantage of this channel in CF, compensating for the absence of functional CFTR.

Although there are several arguments supporting both sides, many studies relied on rather unspecific (possibly affecting other TMEM16A-related effects, e.g., cell proliferation) and low-potency TMEM16A modulators to draw conclusions on the effect of this channel in CF. The identification of novel regulators of TMEM16A can provide meaningful information on the possible applications of this protein as a therapeutic target.

While TMEM16A was described to localize to the apical PM of airway epithelial cells, it is present at the cell surface at low levels, particularly in CF airways.<sup>29</sup> Our hypothesis is that TMEM16A PM levels can be pharmacologically stimulated by modulating its (yet unknown) traffic regulators, ideally also potentiating the channel activity independently of  $\text{Ca}^{2+}$ . The goal of the present study was thus to identify TMEM16A regulators as potential drug targets for novel (“mutation-agnostic”) therapies for CF. Using high-throughput microscopy screens (HTS), we have identified 262 candidate TMEM16A modulators (179 siRNAs enhanced and 83 decreased TMEM16A traffic), being G-protein coupled receptors (GPCRs) enriched on the primary hit list. Among hits in the latter group, we have functionally validated ADRA2C and CXCR3, two G-protein coupled receptors (GPCRs), as potent modulators of TMEM16A trafficking and function. Antagonists of these GPCRs can thus be used to improve  $\text{Cl}^-$  secretion in people with CF, regardless of their CFTR mutations.

## Results

### Identification of TMEM16A traffic regulators by high-content siRNA screening

Using a highly specific TMEM16A antibody to stain cryosections of human airways (CF and non-CF), we have previously shown that there is TMEM16A at the apical surface of epithelial cells of CF airways, albeit at low levels.<sup>29</sup> The same

was observed in cellular models, namely in CFBE cells expressing F508del-CFTR, which display significantly reduced PM expression of TMEM16A when compared to wt-CFTR expressing cells.<sup>30</sup> These data emphasize the need to identify TMEM16A traffic regulators that promote its traffic to the cell surface in the absence of CFTR expression, in order to use this Cl<sup>-</sup> channel as an alternative drug target to compensate for the loss of CFTR-mediated Cl<sup>-</sup> transport in CF.

We have previously generated a cell model expressing double tagged TMEM16A (CFBE 3HA-TMEM16A-eGFP cells) and used it to develop, optimize and validate a screening platform to identify TMEM16A traffic regulators.<sup>29,31</sup> Using this tool, we performed here a high-content siRNA screen to assess the effect of knocking down 691 genes on TMEM16A traffic to the PM (Figure 1(A, B)). This siRNA library comprised siRNAs that: (1) enhance F508del-CFTR PM expression; (2) interact with CFTR; (3) or are involved in general protein trafficking (Amaral lab, unpublished data). The rationale for testing such set of siRNAs was two-fold, firstly to increase TMEM16A PM expression and consequently increase the potential for Cl<sup>-</sup> secretion; and secondly, by targeting these genes in F508del-CFTR expressing cells, besides TMEM16A, CFTR-mediated Cl<sup>-</sup> secretion would also be enhanced. Nonetheless, the screen was performed in CFTR-null cells (CFBE 41o-), to enable the identification of TMEM16A traffic enhancers independently of CFTR. As a negative control, a non-targeting siRNA ("siNEG1") was used. This primary traffic screen identified 262 regulators of TMEM16A traffic: 179 inhibitor genes, i.e., targeted by siRNAs enhancing TMEM16A traffic, and 83 enhancer genes, i.e., targeted by siRNAs inhibiting TMEM16A traffic (Figure 1(A, B), Dataset S1(A, B)).

Since the main goal in CF therapies is to increase anion secretion, we focused on the 179 siRNAs augmenting TMEM16A PM expression for further validation. Representative images obtained for TMEM16A traffic enhancers are shown in Figure 2 (A).

Analysis of these 179 genes using the Gene Ontology Bioinformatics Resource,<sup>32,33</sup> employing a high classification stringency, identified as most important biological processes: (i) regulation of transcription; (ii) G-protein coupled receptor (GPCR) signalling; (iii) protein phosphorylation; (iv) inflammatory response; and (v) negative regulation of cell proliferation.

### Secondary screen: Functional validation of TMEM16A traffic hits

Next, we aimed to assess how the knockdown of the 179 genes affected TMEM16A function using the halide-sensitive (HS)-YFP assay upon ATP-stimulation, as previously described<sup>34</sup> (Figure 1 (C)). We used HEK cells stably expressing TMEM16A and a HS-mutant (YFP-H148Q/I152L)

form of YFP (HEK-TMEM16A-YFP) and analysed the rate of iodide (I<sup>-</sup>) uptake after siRNA knockdown of target genes by calculating the slope of the curves after ATP stimulation.

The knockdown of 20 out of the 179 genes significantly increased the rate of ATP stimulated I<sup>-</sup> transport into the cells, as determined by the steeper slopes observed in the YFP fluorescence decay curves (Figure 2(B, C), Dataset S1(C)). The ATP-mediated YFP-quenching is essentially accomplished by TMEM16A alone since, in the presence of an siRNA targeting TMEM16A (Figure 2(B)), there is a substantially reduced effect. Accordingly, we can confirm that these siRNAs increase TMEM16A function (Figure 2(B, C)).

Out of the 20 TMEM16A regulators, we selected the top 6 hits for mechanistic validation (Table 1) based on several factors, namely: (i) their scores are positive and consistent in both screens; (ii) they are druggable by specific inhibitors (e.g., receptors and kinases); (iii) they are biologically relevant, as their knockdown does not appear to have deleterious/pleiotropic effects on cells; and (iv) GPCRs have a strong relationship with TMEM16A.<sup>30</sup> We confirmed the expression of the 6 selected genes in both CFBE and HEK cells by PCR (Figure S1, Table S1).

To further functionally validate these 6 hits, the effects of the respective siRNAs on TMEM16A function were first evaluated by whole-cell patch-clamp, where TMEM16A was activated using the Ca<sup>2+</sup> ionophore ionomycin (Figure 3). We considered that the use of ATP for TMEM16A activation could be disadvantageous in this case due to its possible interactions with the GPCRs identified as hits (namely through purinergic receptors), therefore masking the real regulatory effects on TMEM16A. Therefore, we stimulated the cells with ionomycin. Experiments were performed in CFBE cells stably expressing F508del-CFTR (CFBE F508del-CFTR), which endogenously express TMEM16A, transfected with siRNAs targeting each of the 6 selected hits. Two siRNAs, targeting ADRA2C and CXCR3 ( $\alpha$ 2C-adrenergic receptor [ $\alpha$ 2C-R], and C-X-C chemokine receptor type 3, respectively), significantly increased Ca<sup>2+</sup>-activated currents at larger depolarizing currents, when compared to the non-targeting control (siNEG1) (Figure 3). Notably, no siRNA affected the cAMP-activated currents (IBMX + Forskolin), therefore showing no direct effects on F508del-CFTR function (Figure S2).

To confirm that the increase in TMEM16A function observed by knocking down ADRA2C and CXCR3 is not unspecific, such as due to an increase in the concentration of intracellular Ca<sup>2+</sup> ([Ca<sup>2+</sup>]<sub>i</sub>), total [Ca<sup>2+</sup>]<sub>i</sub> was measured using a FURA2-AM probe (Figure S3). The knockdown of these GPCRs did not alter [Ca<sup>2+</sup>]<sub>i</sub>, neither basal

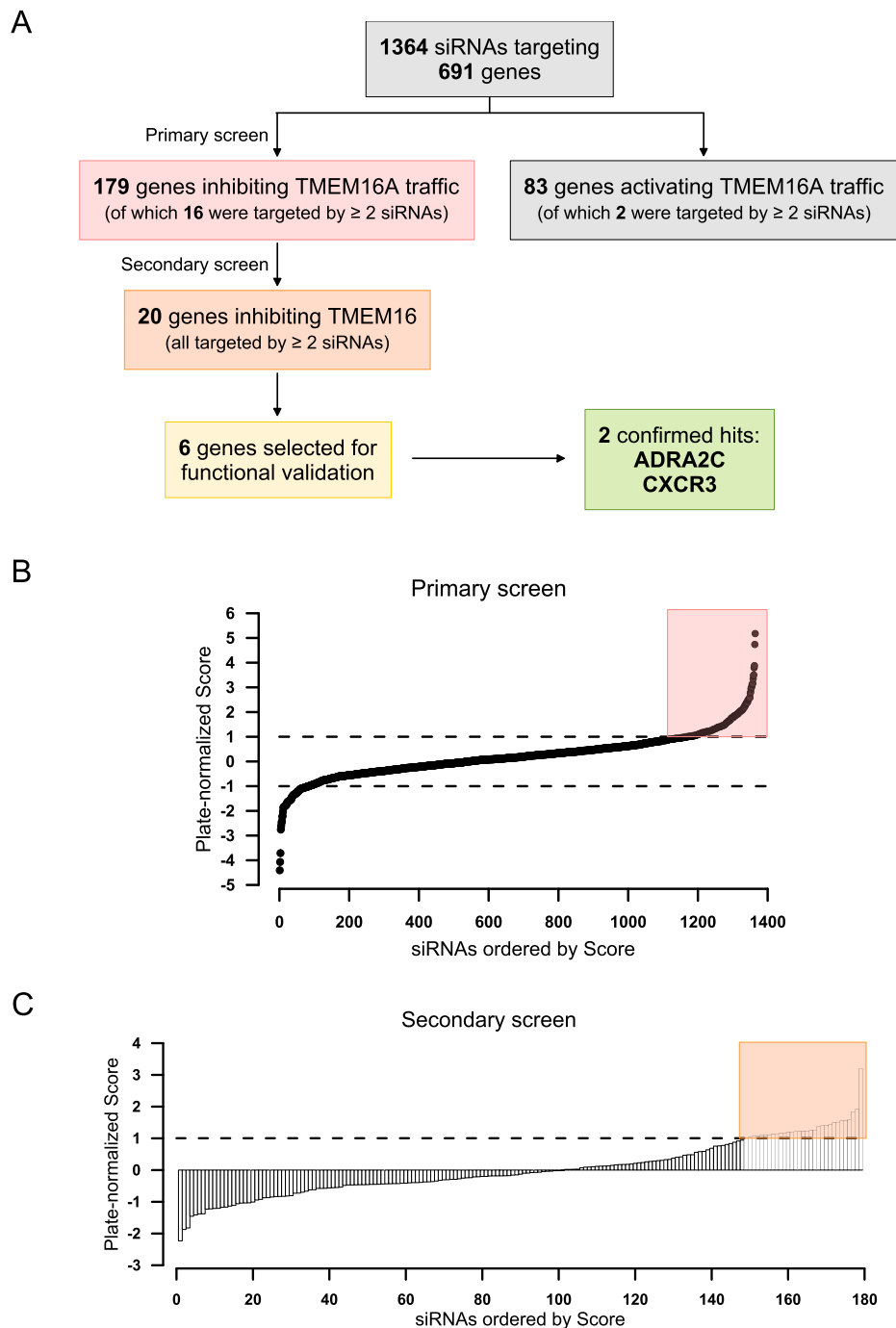


**Figure 1. Overview of the screen data.** (A) Workflow showing the different steps in the primary and secondary screens and the number of hit genes found in each step. (B) Distribution of averaged scores obtained for every siRNA in the primary TMEM16A traffic screen. siRNAs with scores above +1 (red shade) were considered as TMEM16A traffic enhancers (inhibitory genes) and with score below  $-1$  were considered TMEM16A traffic inhibitors (enhancer genes). (C) Distribution of averaged scores obtained for every siRNA in the secondary screen. siRNAs with scores above +1 (orange shade) were considered as enhancers of TMEM16A function.

nor after ionomycin stimulation. Interestingly, their knockdown seems to decrease the  $[Ca^{2+}]_i$  peak (and plateau) observed after ATP stimulation. These data suggest that the increase in TMEM16A function observed by knocking down ADRA2C or CXCR3 is not caused by an increase

in  $[Ca^{2+}]_i$ , but instead by increased TMEM16A PM expression, pointing these genes as suitable drug target candidates to enhance  $Cl^-$  secretion in CF. These data, however, do not exclude an undetectable increase in localized  $[Ca^{2+}]_i$ , namely in microdomains located close to the PM.

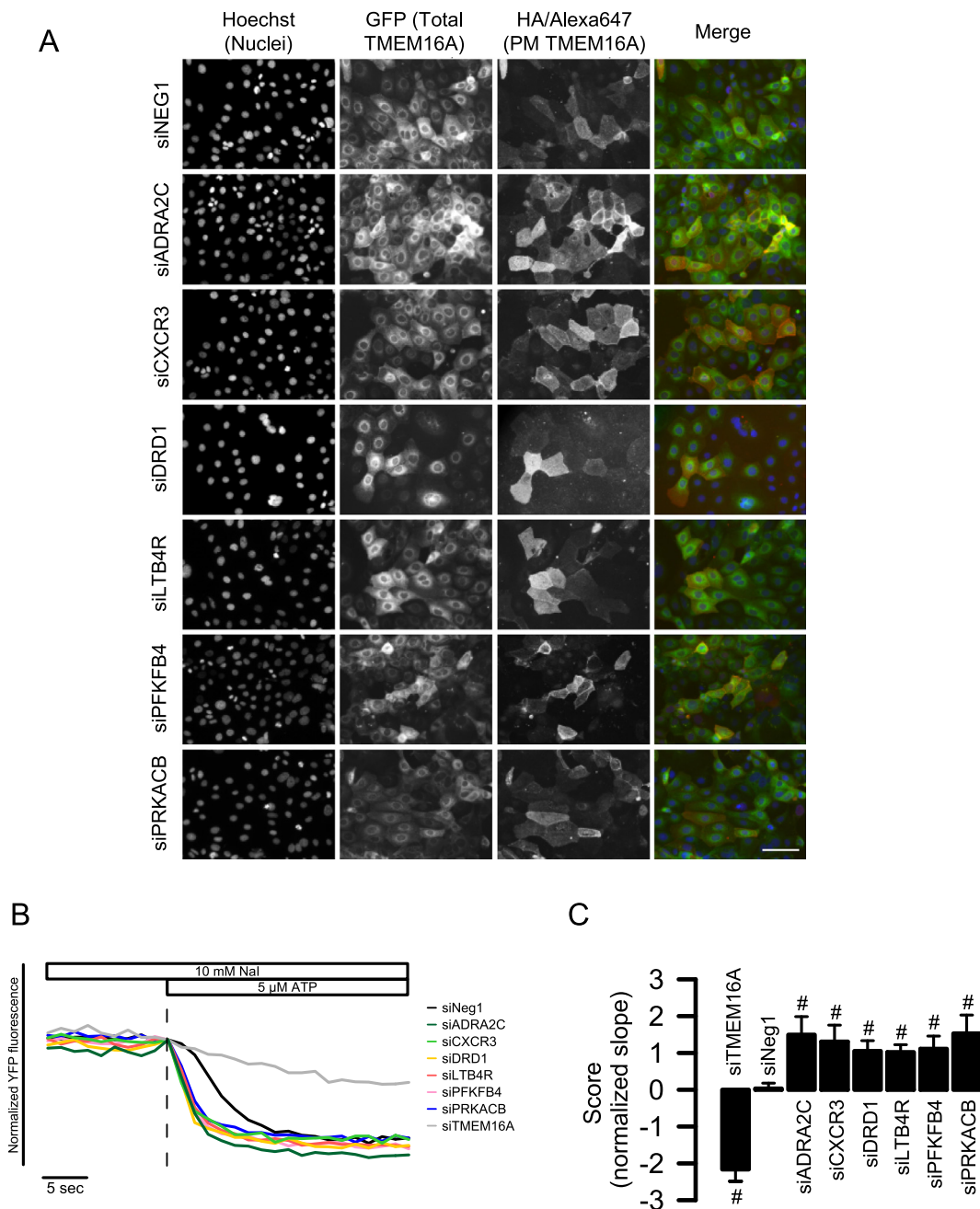


**Figure 2. Summary of the TMEM16A trafficking and functional screens.** (A) Representative widefield epifluorescence microscopy images obtained for the TMEM16A traffic screen using siRNAs targeting the selected genes ( $n = 4$ ) in CFBE 3HA-TMEM16A-eGFP cells. Cell imaging was performed with (automated) widefield epifluorescence microscope with a Scan<sup>R</sup> software (Olympus Biosystems) with a 10 $\times$  UPlanApo objective (Olympus). Scale bar: 50  $\mu$ m. (B) Representative ATP-induced (5  $\mu$ M) YFP-quenching curves obtained by knocking down the selected genes in HEK-TMEM16A-YFP cells. (C) Average of the normalized scores obtained for the selected hits in the YFP-quenching validation screen. Data are represented by mean  $\pm$  SEM ( $n = 4$ ). #Significant difference when compared with the negative control siNEG1 ( $p < 0.05$ ; unpaired  $t$ -test).

### Regulation of TMEM16A by G<sub>i</sub>-Protein coupled receptors ADRA2C and CXCR3

Since knocking down ADRA2C or CXCR3 significantly enhances endogenous TMEM16A function (Figure 3), next we aimed to confirm

whether this effect on endogenously expressed TMEM16A also resulted from increased trafficking. Indeed, TMEM16A immunostaining in CFBE F508del-CFTR cells showed a significant increase in its PM expression after transfection

Table 1 Primary and secondary screen hits selected for mechanistic validation.

Hits selected for validation	Gene name
ADRA2C	Adrenoceptor alpha 2C
CXCR3	C-X-C motif chemokine receptor 3
DRD1	Dopamine receptor D1
LTB4R	Leukotriene B4 receptor
PFKFB4	6-Phosphofructo-2-kinase/fructose-2,6-biphosphatase 4
PRKACB	Protein kinase cAMP-activated catalytic subunit beta

with siRNAs targeting ADRA2C or CXCR3 (Figure 4 (A, B)).

To understand how ADRA2C and CXCR3 regulate TMEM16A, we evaluated TMEM16A protein expression by Western Blot (WB) after knocking down these genes in CFBE F508del-CFTR cells. TMEM16A expression appears to be increased with the knockdown of ADRA2C, while no changes were observed with siCXCR3, when compared to siNEG1 (Figure 4(C–H)). Importantly, only the expression of the glycosylated form<sup>30</sup> of

TMEM16A (i.e., putatively the PM form) was significantly increased when ADRA2C was knocked down. These results reinforce the evidence that the knockdown of ADRA2C is increasing TMEM16A PM expression, either by promoting its anterograde traffic or by stabilizing it at the cell surface. Additionally, the knockdown of ADRA2C or CXCR3 did not affect F508del-CFTR expression (Figure 4(C, D, F, G)).

To analyse the opposite effects on TMEM16A trafficking and function, we overexpressed the

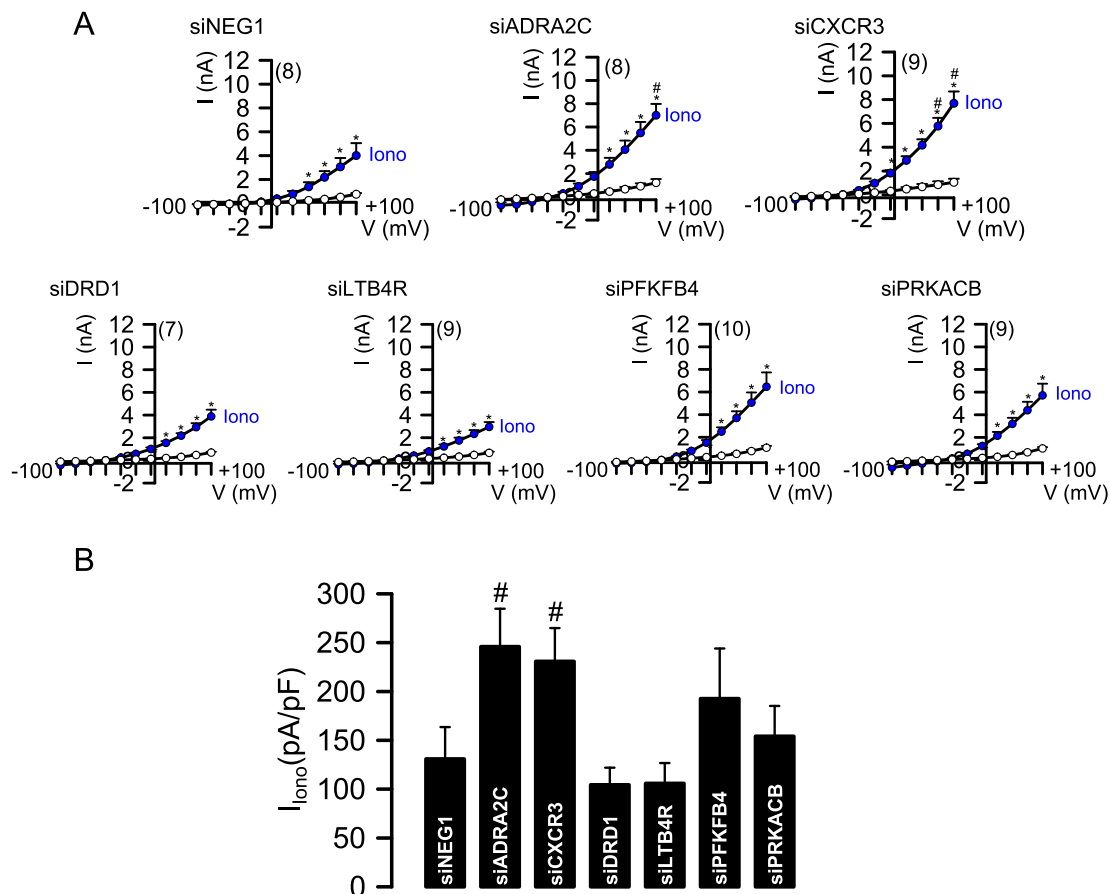


**Figure 3. Validation of hits in CFBE F508del-CFTR cells that endogenously express TMEM16A by whole-cell patch clamp.** (A) Whole cell currents obtained in siRNA-transfected cells (current/voltage (I/V) curves) activated by ionomycin (Iono; 1  $\mu$ M). The number of cells (n) measured in each condition is shown in each graph. (B) Summary of Iono-induced currents with different siRNA treatments, calculated at +100 mV. Data represented as mean  $\pm$  SEM. \*Significant current activation ( $p < 0.05$ ; paired  $t$ -test). #Significant difference when compared with the negative control siNEG1 ( $p < 0.05$ ; unpaired  $t$ -test).

ADRA2C or CXCR3 receptors with either no tags, or with an mCherry tag at the C-terminus of each protein. Even without ligand stimulation, the overexpression of ADRA2C and CXCR3 in CFBE F508del-CFTR cells decreased the trafficking of endogenously expressed TMEM16A (Figure 5(A, B)). Likewise, TMEM16A function, measured by whole-cell patch clamp, was strongly reduced after overexpression of either ADRA2C or CXCR3 (Figure 5(C–E)). As we confirmed that these GPCRs do not affect purinergic receptor signalling (Figure S3), and because it is known that receptor-dependent activation of TMEM16A is more efficient than stimulation by elevating  $[Ca^{2+}]_i$ ,<sup>11,30</sup> we used ATP to activate TMEM16A in further experiments. Agonist stimulation of overexpressed ADRA2C and CXCR3 (with 10  $\mu$ M clonidine or 100 ng/mL CXCL11, respectively) did not further decrease TMEM16A function (Figure S4).

These results were also validated in a system expressing heterologous TMEM16A, namely HEK cells co-transfected with TMEM16A and ADRA2C or CXCR3. In these cells, TMEM16A traffic to the PM was significantly reduced vs mock-transfected cells (Figure 5(F, G)). TMEM16A function was also compromised upon overexpression of ADRA2C or CXCR3, as YFP-quenching data in HEK-TMEM16A-YFP showed a strongly diminished  $I^-$  uptake in cells overexpressing ADRA2C or CXCR3 when compared to mock-transfected cells (Figure 5(H, I)).

### TMEM16A function and cAMP levels

Both the ADRA2C and the CXCR3 genes encode  $G_i$  protein-coupled receptors, being adrenoceptor alpha 2c ( $\alpha 2C-R$ ) activated by catecholamines (e.g., epinephrine or norepinephrine),<sup>35</sup> and c-x-c motif chemokine receptor 3 (CXCR3) by chemokines CXCL9, CXCL10 or CXCL11.<sup>36</sup> Since receptor stimulation leads to the inhibition of adenylyl cyclase (AC) and consequently blocks the synthesis of the second messenger cAMP from ATP,<sup>37</sup> we can infer that knocking down these genes (and consequently inhibiting  $G_i$ ) can increase intracellular cAMP levels. On the other hand, receptor overexpression could lead to AC inhibition, thus lowering intracellular cAMP levels ( $[cAMP]_i$ ). Moreover, due to crosstalk between  $Ca^{2+}$  and cAMP signalling reported before,<sup>30</sup> it is expected that higher concentrations of cAMP also lead to an increase in  $Ca^{2+}$ -activated  $Cl^-$  currents. We thus postulated that the observed effects of these  $G_i$  protein-coupled receptors on TMEM16A function could be related to changes in cAMP levels.

To confirm this hypothesis, we started by measuring  $[cAMP]_i$  in HEK cells transfected with either ADRA2C or CXCR3, using a fluorescence resonance energy transfer (FRET)-based Epac cAMP sensor (YFP-Epac-CFP).<sup>38,39</sup> The exchange protein directly activated by cAMP (Epac) sensor allows for a quantitative analysis of changes in

$[cAMP]_i$ , where increases in the ratio CFP/YFP indicate higher concentrations of cAMP (see Methods). No differences were observed in basal cAMP levels in cells transfected with either ADRA2C or CXCR3 (Figure S5(A)). Inhibition of  $G_i$  protein-coupled signalling pathways by pertussis toxin (PTX)<sup>40</sup> strongly increased intracellular cAMP, thus augmenting the FRET signal. Cells overexpressing either ADRA2C or CXCR3 showed significantly higher cAMP levels when compared to control (mock-transfected) cells after PTX incubation. AC stimulation by forskolin led to the same levels of intracellular cAMP in all conditions. Finally, incubation with phosphodiesterase inhibitor IBMX did not further increase cAMP levels, reflecting a near-complete saturation of cAMP binding to Epac (Figure S5(A)). These data suggest that, even though basal  $[cAMP]_i$  is unaltered in cells transfected with ADRA2C or CXCR3,  $G_i$  protein-coupled signalling is more active than in control cells, even without ligand stimulation.

Thus, to determine if this increase in  $G_i$  protein-coupled signalling activation is reflecting on TMEM16A function, we incubated HEK-TMEM16A-YFP cells with compounds that increase  $[cAMP]_i$ . If the overexpression of the GPCRs ADRA2C and CXCR3 were inhibiting TMEM16A function due to the inhibition of cAMP synthesis, then adding exogenous cAMP would likely restore TMEM16A function in ADRA2C/CXCR3-transfected cells. After incubating cells for 2 h with compounds that increase  $[cAMP]_i$ , namely PTX, the membrane permeable cAMP analogue 8-bromo-cAMP, or forskolin (with or without costimulation with IBMX), we observed an increase in the ATP-induced YFP quenching in HEK-TMEM16A-YFP cells (Figure S5(B, C)). Yet, the increase in ATP-induced YFP quenching was proportional in all conditions – either in cells transfected with an empty vector or with ADRA2C or CXCR3 – being the YFP quenching always higher in the control cells (mock), as observed before (Figure 5).

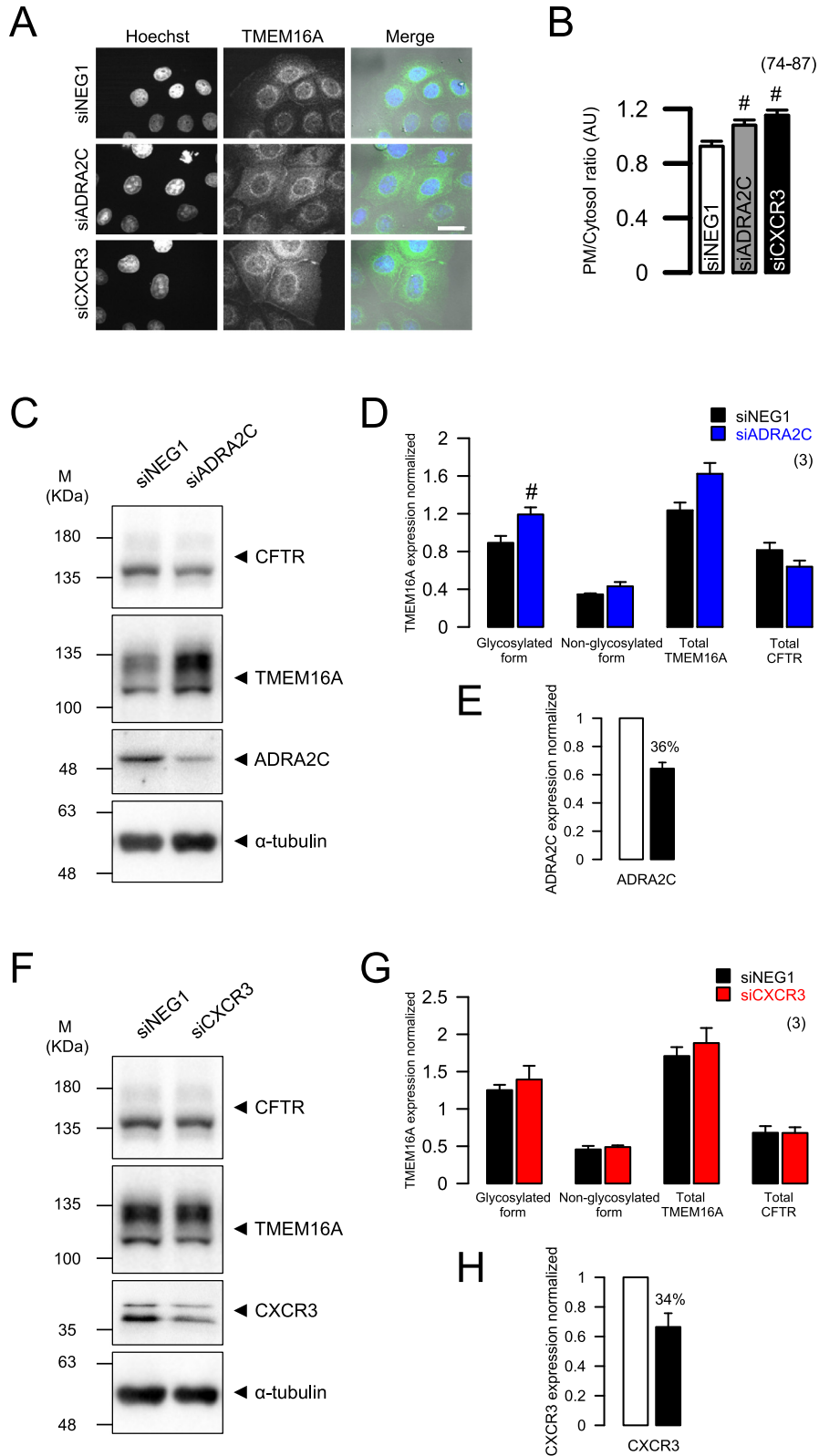
Altogether, these data suggest that although the overexpression of ADRA2C or CXCR3 increase  $G_i$  protein-coupled signalling, and the rise in cAMP levels leads to higher TMEM16A activity, possibly by a crosstalk in cAMP and  $Ca^{2+}$  signalling pathways, the regulation of TMEM16A by these GPCRs is most likely not directly due to changes in cAMP concentration.

### ADRA2C and CXCR3 regulate TMEM16A expression by influencing its PM stability

To further investigate the mechanism of action (MoA) of the identified hits, we assessed the effects of combining siADRA2C and siCXCR3 with siRNAs targeting known components of the COPI trafficking machinery (COPB1 and COPZ1) – which were hits in the present study, and had already been described as modulators of TMEM16A PM expression<sup>29,41</sup> – or AP2M1 (Adap-

tor Related Protein Complex 2 Subunit  $\mu$ ), a subunit of AP-2 clathrin adaptor, an essential component of the endocytic clathrin coat,<sup>42</sup> on the PM localization of TMEM16A. The combination of siADRA2C or

siCXCR3 with siCOPB1 and siCOPZ1 were additive to the effect of the knockdown of the receptors alone by further increasing TMEM16A PM expression (Figure 6(A, B)). Interestingly, the simultane-



ous knockdown of ADRA2C and CXCR3 is not additive, and even decreased the effect of the separate knockdown of these GPCRs (although the difference is not statistically significant), suggesting that their MoA is similar. Finally, although the knockdown of AP2M1 did not significantly increase TMEM16A PM expression (score = 0.843), when combining the siRNAs targeting AP2M1 and one of the GPCRs (ADRA2C or CXCR3), the potentiation of TMEM16A PM expression observed with the individual knockdown of the receptors is abolished (Figure 6(A, B)). Thus, these data suggest that ADRA2C and CXCR3 are influencing TMEM16A PM expression in a post-Golgi process, probably by destabilizing it at the PM and/or enhancing its endocytosis (Figure 7).

## Discussion

### Searching for new therapies for all: TMEM16A as an alternative Cl<sup>-</sup> channel in CF

Recent advances in drug development have made it possible to deliver an effective therapy for the majority of CF patients (~80–85%). Yet, the remaining ~20% with mutations that are not effectively corrected by the available modulators justify the need to search for new therapies suitable for all individuals with CF, regardless of their CFTR genotype. Targeting alternative Cl<sup>-</sup> channels might just be an effective way of doing so.

While there is still some controversy on whether TMEM16A should be activated or inhibited in the context of CF, it is nevertheless essential to understand the multiple cellular roles of TMEM16A and how this channel is regulated before using it as a therapeutic target. Thus, the TMEM16A traffic screening data generated here constitute a highly valuable tool, as they shed light on the global regulatory network of TMEM16A. Indeed, in a recent study using cancer cell lines, we showed how the traffic screen can also be useful for the identification of TMEM16A inhibitors, namely in the context of head and neck cancers.<sup>43</sup> Aberrant upregulation of TMEM16A has been reported in various types of cancers, including gastro-intestinal squamous cancer,<sup>44</sup> head and neck squamous cell carcinoma,<sup>45</sup> breast cancer,<sup>46</sup> and lung cancer,<sup>47</sup> being generally linked with a

poor prognosis.<sup>48</sup> Interestingly, in some cancer cell lines, although TMEM16A expression is highly upregulated, the Ca<sup>2+</sup>-activated currents are not increased. This may be explained by the fact that TMEM16A is mostly localized intracellularly and not at the cell surface.<sup>49</sup> Also, TMEM16A upregulation has been shown to occur under conditions that also stimulate cell proliferation,<sup>25</sup> being therefore not clear if TMEM16A aberrant expression in cancer is a cause or a consequence of increased proliferation.

Concerns about the effects of activating TMEM16A on bronchoconstriction have also been raised.<sup>24</sup> However, a new TMEM16A potentiator, ETX001, increased Cl<sup>-</sup> secretion and ASL height and promoted MCC in primary CF bronchial epithelial cells in in vivo sheep models, while showing no effects on airway smooth muscle contraction.<sup>26</sup> This compound is currently in phase I clinical trials, and the results will be fundamental to understand the potential of using TMEM16A as an alternative Cl<sup>-</sup> channel in CF.

Furthermore, it is important to note that TMEM16A and CFTR are intimately connected. The knockout of TMEM16A in mouse airways and intestine, and also in human cells, eliminates both Ca<sup>2+</sup> and cAMP-activated Cl<sup>-</sup> currents.<sup>28</sup> The expression of CFTR at the PM is also compromised in the absence of TMEM16A. Moreover, we have previously reported that there is a significant overlap between cAMP-dependent and Ca<sup>2+</sup>-activated Cl<sup>-</sup> currents due to the crosstalk of compartmentalized signalling molecules.<sup>30</sup> We found that in the absence of PM-localized CFTR, a significant portion of the cAMP-activated Cl<sup>-</sup> current is due to TMEM16A.<sup>30</sup> Additionally, we have recently observed in several cell models that TMEM16A and TMEM16F, another PM-localized TMEM16 paralogue, are essential for CFTR function and insertion at the PM, as well as for F508del-CFTR correction by its modulator drugs VX-809 + VX-770.<sup>50</sup>

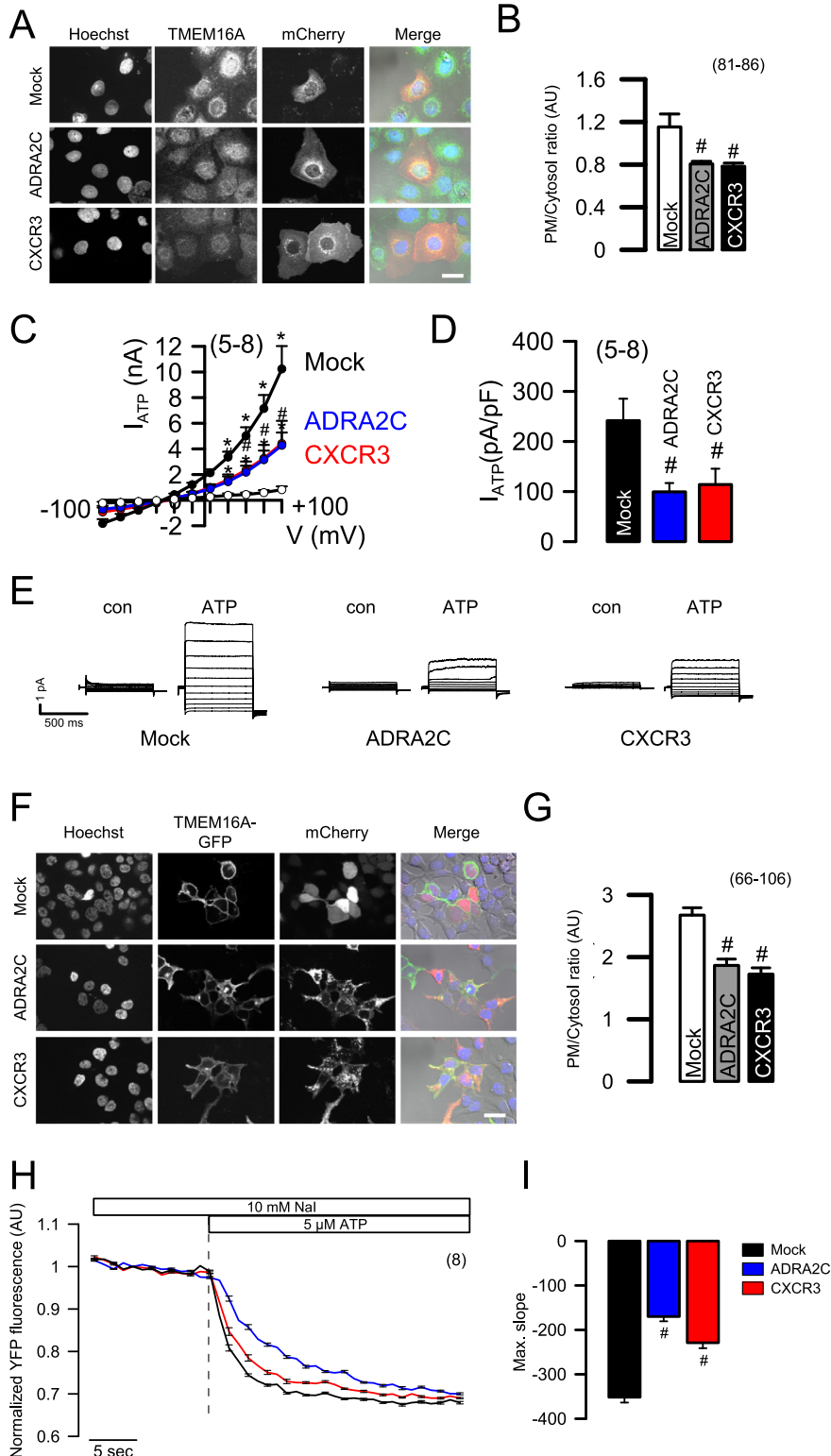
### ADRA2C and CXCR3 as regulators of TMEM16A PM expression and function

In the present study, because we focused on increasing the PM expression of TMEM16A to potentiate Cl<sup>-</sup> secretion in CF cells, we searched

**Figure 4. Effects of ADRA2C or CXCR3 knockdown on endogenous TMEM16A expression and function.** (A) Representative fluorescence microscopy images of endogenous TMEM16A in CFBE F508del-CFTR cells transfected with siNEG1 or siRNAs targeting ADRA2C or CXCR3 and respective quantification in (B). (C) Western Blot of CFBE F508del-CFTR cells transfected with a siRNA targeting ADRA2C. siNEG1 non-targeting siRNA was used as control. (D) Quantification of TMEM16A and CFTR expression detected in (C), showing only a significant difference in glycosylated TMEM16A expression after transfection with siADRA2C when compared to the control. (E) Quantification of ADRA2C knockdown. (F) Western Blot of CFBE F508del-CFTR cells transfected with a siRNA targeting CXCR3 or siNEG1 non-targeting siRNA as control. (G) Quantification of TMEM16A and CFTR expression detected in (F). (H) Quantification of CXCR3 knockdown. Mean ± SEM (number of cells measured). #Significant difference when compared with the negative control ( $p < 0.05$ ; unpaired  $t$ -test).

for modulators that improved its traffic and not its total expression levels, while also not increasing  $Ca^{2+}$  levels inside the cell. In our HTS, among the 691 genes screens, we identified 262 hits putative regulators (179 siRNAs enhancing and 83 decreasing) of TMEM16A PM traffic (38% hit

rate). This number is quite high, but in order to avoid having false negatives in the primary screen, we considered all genes with at least one siRNA with a score above +1. However, only 20 hits out of 179 putative inhibitor genes were confirmed during the secondary screen, validating



their role on TMEM16A function (11% validation rate). This validation rate is actually lower than the one reported in data from multiple high-content screens, which have estimated that ~30% of siRNAs effects can be confirmed.<sup>51–53</sup> The reason for this may be two-fold: (1) our parameters to consider genes as hits were more stringent in the validation screen; (2) different cell lines express different genes, and consequently some of the hits obtained in CFBE cells (traffic screen) may not be expressed in HEK cells (functional assay).

ADRA2C and CXCR3 are negative regulators of TMEM16A PM expression and function in a CF relevant cellular model (CFBE cells). While these data highlight again the importance of this screening platform for unravelling the TMEM16A interactome and for drug discovery, they demonstrate that the two GPCRs identified, when blocked, might enhance TMEM16A-mediated  $\text{Cl}^-$  secretion in all individuals with CF, thus being potential novel targets for CF therapies.

ADRA2C and CXCR3 encode  $G_i$  protein-coupled receptors ( $\alpha_{2C}$ -adrenergic receptor [ $\alpha_{2C}$ -R], and C-X-C chemokine receptor type 3, respectively). Upon receptor stimulation, the  $\alpha_i$  subunit of the heterotrimeric G protein is activated and dissociated from the  $\beta\gamma$  dimer, leading to the inhibition of AC, and consequently blocking the synthesis of the second messenger cAMP from ATP<sup>37</sup>. Hence, our first hypothesis was that inhibition (or in this case silencing) of GPCRs would lead to an increase in cAMP levels, which could be the cause of TMEM16A increased activity, due to the crosstalk between  $\text{Ca}^{2+}$  and cAMP signalling pathways. Accordingly, receptor overexpression would decrease  $[\text{cAMP}]_i$ , also diminishing TMEM16A activity. Our data with ADRA2C or CXCR3 overexpression, however, showed no differences in basal cAMP levels when compared to control cells, while demonstrating a strong increase in  $[\text{cAMP}]_i$  when  $G_i$  was inhibited by PTX, indicating that  $G_i$  is more active in cells overexpressing ADRA2C or CXCR3. These data suggest that these GPCRs, when overexpressed, are either active without ligand stimula-

tion or they can be activated due to the presence of receptor agonists in the culture medium, which is true at least for ADRA2C, as epinephrine and/or norepinephrine are present in foetal bovine serum (FBS) used in cell culture.<sup>54</sup>

In fact, our microscopy experiments with mCherry-tagged ADRA2C and CXCR3 show a great number of internalized receptors, which then co-localize with TMEM16A intracellularly, suggesting ligand-induced desensitization/internalization of these GPCRs. Also, our data show that agonist stimulation of ADRA2C (with clonidine) or CXCR3 (with CXCL11) does not further inhibit TMEM16A activity. Functional studies of TMEM16A under the presence of cAMP-increasing agents confirmed that the effects of ADRA2C and CXCR3 on TMEM16A traffic and function are not caused by changes in global cAMP levels. Small, localized changes, however, cannot be excluded.

Although inhibition of AC is the main coupling pathway for the  $\alpha_2$ -adrenergic receptors, studies showed that  $\alpha_{2A}$ -R (another  $\alpha_2$  receptor subtype) agonist stimulation leads to an increase in  $[\text{Ca}^{2+}]_i$  that involves activation of phospholipase C (PLC) by  $G_{\beta\gamma}$  subunits.<sup>55</sup> Likewise, agonist stimulation of CXCR3 leads to  $[\text{Ca}^{2+}]_i$  increase in T cells in a PLC-dependent process.<sup>56</sup> Additionally, studies in rat aorta suggested that increased cAMP (which is expected with ADRA2C/CXCR3 knockdown) depletes intracellular  $\text{Ca}^{2+}$  stores through activation of Protein Kinase A (PKA) and EPAC, thus reducing the amount of  $\text{Ca}^{2+}$  released by  $\text{IP}_3$ -generating agonists, such as ATP.<sup>57</sup> This is a possible explanation for the lower  $[\text{Ca}^{2+}]_i$  upon ATP stimulation observed in siRNA-transfected cells, and for the small (not significant) increase in basal  $[\text{Ca}^{2+}]_i$  in these cells.

Altogether, these data suggest that the increase in TMEM16A PM expression and function observed with the knockdown of ADRA2C and CXCR3 are not caused by intracellular  $\text{Ca}^{2+}$  nor cAMP increase. Instead, the two GPCRs seem to interact with TMEM16A in a similar way, likely by destabilizing it in a post-Golgi event, either by

### Figure 5. Effects of ADRA2C or CXCR3 overexpression on TMEM16A expression and function.

(A) Representative images of endogenous TMEM16A staining in CFBE F508del-CFTR cells overexpressing mCherry-tagged ADRA2C or CXCR3 and respective quantification in (B). Images were acquired with an Axiovert 200 microscope equipped with ApoTome and AxioVision (Zeiss, Germany), with a 63 $\times$  objective. Scale bars = 30  $\mu\text{m}$  (number of cells measured). (C, D) Current/voltage curves and corresponding summary of ATP-induced currents in CFBE F508del-CFTR cells transfected with ADRA2C, CXCR3 or an empty vector, calculated at +100 mV. (E) Whole cell overlay currents ( $V_c = \pm 100$  mV, steps 20 mV) activated by ATP (100  $\mu\text{M}$ ). (F) Representative fluorescence microscopy images of TMEM16A in HEK cells co-transfected with a mCherry vector or with ADRA2C/CXCR3 tagged with mCherry and respective quantification in (G). Scale bar = 30  $\mu\text{m}$ . The number of cells (n) measured is shown in the graph. (H) ATP-induced YFP quenching curves of HEK-TMEM16A-YFP cells transfected with ADRA2C or CXCR3 and respective slope quantification in (I). Mean  $\pm$  SEM (number of experiments). \*Significant current activation ( $p < 0.05$ ; paired  $t$ -test). #Significant difference when compared with mock-transfected cells ( $p < 0.05$ ; unpaired  $t$ -test).

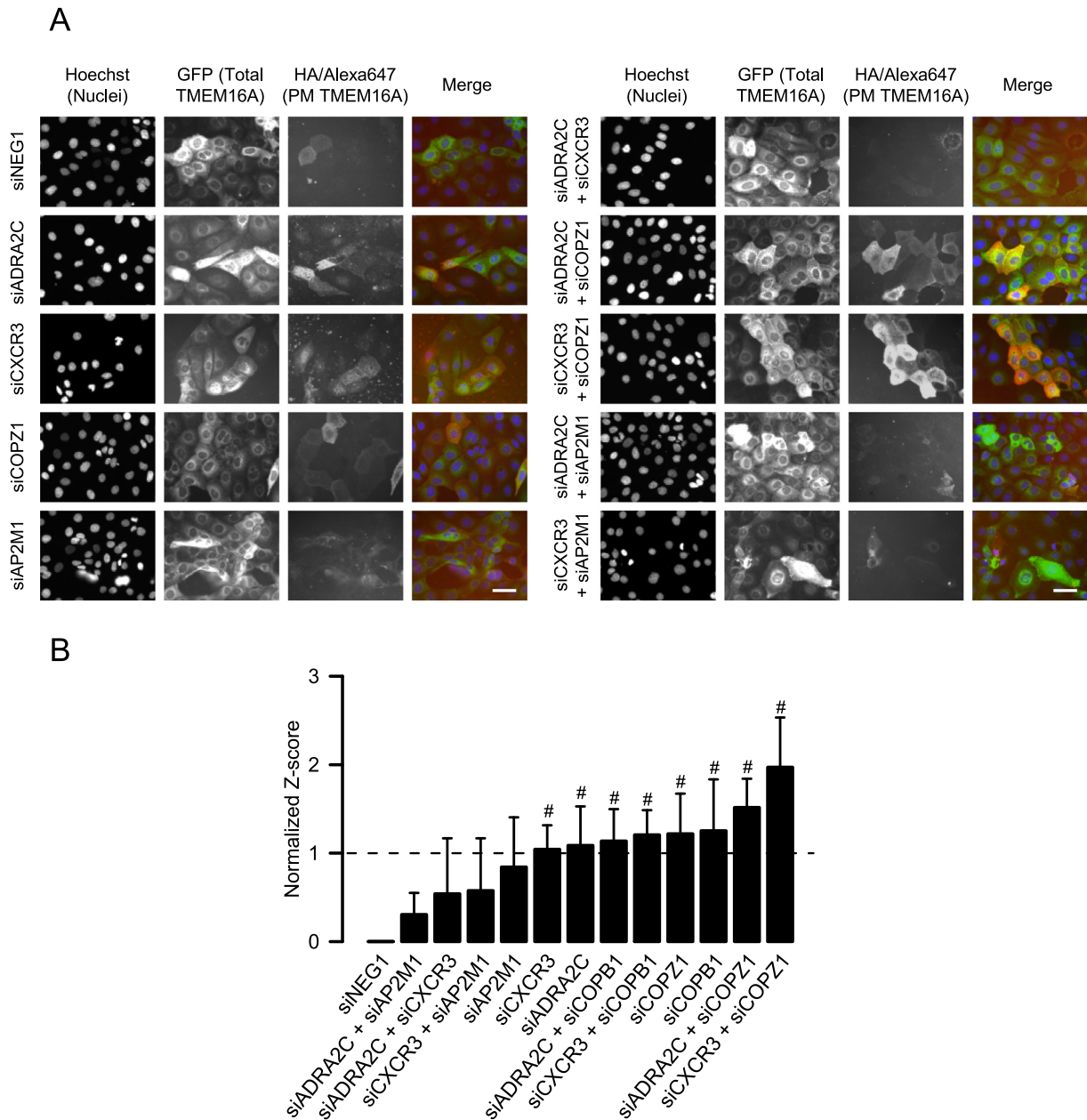


**Figure 6. The effect of knocking down ADRA2C and CXCR3 on TMEM16A PM expression is additive with siCOPB1 and siCOPZ1 but not with siAP2M1.** (A) Representative widefield epifluorescence microscopy images obtained for TMEM16A PM expression using siRNAs targeting the two selected hits (ADRA2C and CXCR3) in combination with other siRNAs involved in endocytosis/trafficking. Cell imaging was performed with a Leica DMI 6000B widefield microscope (objective: 20x water, 0.75 NA; exposure times: Hoechst: 50 ms, GFP: 3 s, Alexa647: 3 s). Scale bar: 30  $\mu$ m ( $n = 4$ ). (B) Average of the normalized scores obtained for TMEM16A PM expression obtained in (A). #Significant difference when compared with siNEG1-transfected cells ( $p < 0.05$ ; unpaired  $t$ -test).

promoting endocytosis or preventing its recycling to the PM (Figure 7). This was confirmed by simultaneously knocking down the GPCR hits and genes involved in the retrograde transport or in clathrin-mediated endocytosis.

The increase in TMEM16A PM expression caused by knocking down ADRA2C or CXCR3 was further augmented by the knockdown of

COPB1 and COPZ1, which mediate traffic within the Golgi and from the cis-Golgi back to the ER (retrograde). Silencing of components of the COPI trafficking machinery had already been shown to promote TMEM16A PM expression.<sup>29</sup> These results suggest that the interaction between the hits and TMEM16A occurs after the latter exits the Golgi (Figure 7).

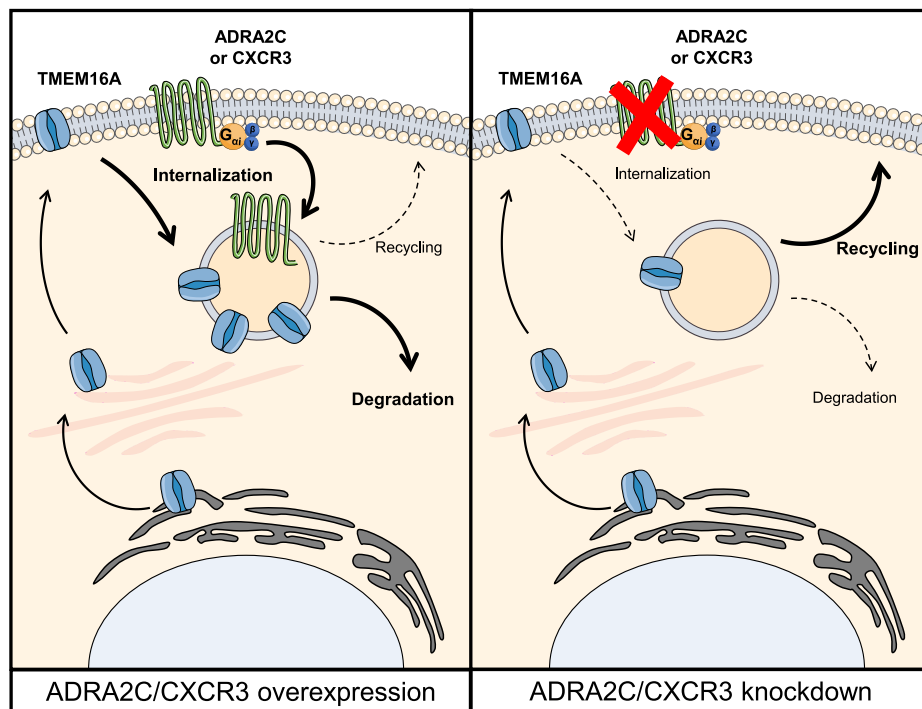


**Figure 7. Model for the regulation of TMEM16A traffic by ADRA2C/CXCR3.**

GPCR signalling is commonly regulated by receptor phosphorylation and internalization, processes which depend on agonist binding. Agonist-bound GPCRs are phosphorylated by GPCR kinases (GRKs), which then bind to arrestin proteins and are internalized.<sup>58</sup> Internalization seems to be important for dephosphorylation and resensitization of GPCRs.<sup>59</sup>  $\alpha_2$  receptors, such as the  $\alpha_2C$ -adrenergic receptor, seem to follow the same mechanism.<sup>60</sup> In contrast, although CXCR3 is also endocytosed after ligand binding, it is not recycled to the PM, being instead degraded after internalization.<sup>61</sup> Therefore, since overexpressed ADRA2C and CXCR3 were partially internalized and co-localized with TMEM16A intracellularly, our interpretation of this data is that TMEM16A is endocytosed together with ADRA2C and/or CXCR3 when they are internalized. Consequently, siRNA knockdown of these GPCRs leads to increased stabilization of TMEM16A at the PM, which is further potentiated when there is more TMEM16A exiting the Golgi (namely after COPB1 and COPZ1 knockdown).

Although not much is known regarding TMEM16A endocytosis and recycling, CFTR is endocytosed in clathrin-coated vesicles, and approximately 50% is recycled back to the PM.<sup>62</sup> Also, we have previously seen that treatment of CFBE cells with brefeldin A (which collapses the Golgi and thus blocks secretory traffic) does not decrease  $Ca^{2+}$ -activated  $Cl^-$  currents nor TMEM16A PM levels up to 24 hours,<sup>30</sup> which indicates that TMEM16A is either following an alternative trafficking route, or, most likely, that it is rapidly recycled to the PM after internalization.

AP-2 is an endocytic adaptor important for cargo uptake in clathrin-mediated endocytosis.<sup>39,63</sup> The knockdown of the subunit  $\mu$  of AP-2 (siAP2M1), did not significantly alter TMEM16A expression at the PM, although its score is close to the hit threshold (score = 0.843). This result might be explained by previous data showing a small but detectable expression of AP-2 in the clathrin coated pits that still form (although in lower amounts) in the siRNA treated cells.<sup>39</sup> Alternatively, TMEM16A might have additional endocytosis routes. However, co-transfection of cells with siAP2M1 and siRNAs targeting either ADRA2C or CXCR3 strongly reduced the effects observed when the siRNAs are employed individually. Other findings suggest that depletion of AP-2 affects endocytic trafficking through the non-clathrin, ADP-ribosylation factor (Arf) 6 regulated pathway, promoting lysosomal targeting and degradation of Arf6-pathway cargo over recycling.<sup>64</sup> Therefore, siAP2M1 might not completely inhibit endocytosis, but instead block TMEM16A recycling to the PM. Consequently, although siADRA2C or siCXCR3 prevent some endocytosis of TMEM16A, simultaneous knockdown of AP2M1 inhibits TMEM16A recycling, eliminating the positive effects of silencing the GPCRs.

## Conclusions

Here we present two GPCRs (ADRA2C and CXCR3) as novel modulators of TMEM16A, which appear to work as destabilizers of TMEM16A at the PM. Uncoupling of TMEM16A membrane sorting from these GPCRs or silencing/blocking

them may be a way of increasing  $\text{Cl}^-$  secretion in CF. However, owing to TMEM16A importance in physiology and pathology, as well as to its therapeutic potential, there is an urgent need to improve our understanding of how TMEM16A contributes to human disease, and to better define drugs and conditions for using this channel as a therapeutic target in CF and other respiratory disorders. We believe that, similarly to what happens with CFTR modulator drugs, CF patients would benefit from a combination of therapies. Namely, the knockdown (and possibly the inhibition) of these GPCRs would increase the PM expression of TMEM16A, and its activation could be further potentiated by compounds such as EXT001 that has been proven to enhance fluid secretion and ASL height in CF-HBE cells, and also mucociliary clearance in ovine models.<sup>26</sup>

## Materials and methods

### Cell culture

Cystic Fibrosis Bronchial Epithelial cells (CFBE) stably overexpressing 3HA-TMEM16A-eGFP were cultured in MEM (Minimum Essential Media) with L-Glutamine supplemented with 10% (v/v) heat inactivated foetal bovine serum (FBS), 400  $\mu\text{g}/\text{mL}$  G418 and 2.5  $\mu\text{g}/\text{mL}$  puromycin. CFBE stably expressing F508del-CFTR were grown in MEM supplemented with 10% FBS and 2.5  $\mu\text{g}/\text{mL}$  puromycin. Human Embryonic Kidney (HEK) 293 T were cultured in DMEM (Dulbecco's Modified Eagle Medium) with 10% FBS, without antibiotics. HEK cells stably expressing halide sensitive (HS)-YFP and TMEM16A were cultured in DMEM supplemented with 10% FBS, 0.5  $\mu\text{g}/\text{mL}$  puromycin and 150  $\mu\text{g}/\text{mL}$  hygromycin B. All cells were cultured at 37 °C in a humidified atmosphere of 5% (v/v)  $\text{CO}_2$ .

### Immunocytochemistry

To identify TMEM16A regulators through the TMEM16A trafficking assay we knocked down 691 genes (Dataset S1A), targeted by 1364 siRNAs previously identified (Amaral lab, unpublished data).

Multi-well plates (BD Falcon) were coated with customized siRNAs pre-mixed with lipofectamine for solid-phase reverse transfection adapted from a previously reported protocol<sup>65</sup> with adjustments also described before.<sup>31</sup> CFBE 3HA-TMEM16A-eGFP cells were seeded on the siRNA coated 384-well plates (50  $\mu\text{L}/\text{well}$ ,  $3 \times 10^3$  cells/well). TMEM16A expression was induced 24 h after seeding with antibiotic-free medium supplemented with 1  $\mu\text{g}/\text{mL}$  doxycycline, and the extracellular HA-tag was immunostained in non-permeabilized cells 72 h after seeding (48 h after Dox induction). Cells were washed in cold PBS with 0.7 mM  $\text{CaCl}_2$  and 1.1 mM  $\text{MgCl}_2$  and incubated 1 h at 4 °C with a

mouse monoclonal anti-HA antibody (Biolegend, 901502). Cells were washed 3x with PBS, incubated 20 min with 3% (w/v) paraformaldehyde (PFA) at 4 °C and transferred to room temperature (RT). After washing, cells were incubated for 1 h with an anti-mouse Alexa Fluor<sup>®</sup> 647 conjugated secondary antibody and Hoechst 33342 (200 ng/mL), and finally washed and incubated with PBS overnight before imaging.

For endogenous TMEM16A stainings, cells were grown on glass coverslips and fixed with methanol and acetone (4:1) for 10 min at -20 °C. After washing 3 times with PBS supplemented with 0.7 mM  $\text{CaCl}_2$  and 1.1 mM  $\text{MgCl}_2$ , cells were blocked with 3% (w/v) bovine serum albumin (BSA) in PBS for 30 min at RT and incubated with the primary antibody DOG1 (Novus Biologicals #NP060513) in 1% BSA overnight at 4 °C. Binding of the primary antibody was visualized by incubation with an anti-rabbit Alexa Fluor<sup>®</sup> 488 conjugated secondary antibody in 1% BSA for 1 h at RT (Invitrogen, A-21206). Nuclei were stained with Hoechst 33342. Cells were mounted on glass slides with mounting medium (DAKO Cytomation, Hamburg, Germany) and examined with an Axiovert 200 microscope equipped with ApoTome and AxioVision (Zeiss, Germany).

### Image acquisition and analyses

Automated cell imaging of 384-well plates was performed with a widefield epifluorescence microscope with a Scan<sup>^</sup>R software (Olympus Biosystems) equipped with motorized stage and a metal halide light source (MT20), a 12-bit  $1344 \times 1024$  pixel resolution C8484 CCD camera (Hamamatsu OrcaFlash4) and a 10x UPlanApo objective (Olympus) and 0.4 of numerical aperture. Exposure times were for Hoechst, eGFP and Alexa Fluor<sup>®</sup> 647 of (ms) 10–20, 500 and 2000, respectively. The Hoechst channel was used for contrast-based autofocus. Filter settings (Excitation wavelengths/excitation band (nm) – Ex, Emission wavelengths/emission band (nm) – Em): Hoechst – Ex 347/50, Em 460/50; eGFP – Ex 470/40, Em 525/50; Alexa 647 – Ex 640/30, Em 690/50.

Image analysis was performed with open source software tools (CellProfiler and R) using specific pipelines appropriate for traffic assays, all as described previously,<sup>29,31</sup> with minor changes. Briefly, the fluorescence quantification of the Alexa 647 channel allowed the determination of TMEM16A PM expression in each cell. After averaging TMEM16A PM expression for all images from the same siRNA treatment, the effect of different siRNAs on TMEM16A traffic was compared with the results obtained with the non-targeting siRNA (siNEG1) treatments, using the following formula:

$$Z - score(x_{plate_i}) = \frac{x_{plate_i} - Average_{siNEG1,plate_i}}{SD_{siNEG1,plate_i}}$$

$SD_{siNEG1}$  is the standard deviation for PM TMEM16A with the treatment with non-targeting siRNA. Significant effects on the PM expression of TMEM16A were considered when the magnitude was larger than the siNEG1 SD. Hence, genes with a score above +1 were considered traffic enhancers, and genes having a score below -1 were considered traffic inhibitors. Additionally, two tailed Student's *t*-tests were performed to quantify statistical significance versus siNEG1.

### YFP-Quenching

HEK-TMEM16A-YFP (expressing the YFP-H148Q/1152L variant)<sup>66</sup> were seeded at a density of  $3 \times 10^4$  cells/well on siRNA-coated 96-well plates. 48 h after seeding, cells were washed once with 20 mM Na-Gluconate solution (in mM: NaCl 120, Na-Gluconate 20, KCl 5, MgCl<sub>2</sub> 1, CaCl<sub>2</sub> 2, Glucose 10, HEPES 10), and placed in the plate reader for measurements (NOVOstar, BMG Labtech). After measuring the baseline fluorescence, cells were incubated with 10 mM NaI solution (final concentrations in mM: NaCl 120, NaI 10, KCl 5, MgCl<sub>2</sub> 1, CaCl<sub>2</sub> 2, Glucose 10, HEPES 10) for 20 s, and then were stimulated with 5 μM ATP (final concentration) for 30 s, to induce I<sup>-</sup> uptake and consequently the quenching of the YFP fluorescence. The experiments were performed at 37 °C, and the excitation and emission wavelengths were, respectively, 485 and 520 nm.

The maximum slope of the curves obtained with the different siRNA treatments was calculated using the BMG LABTECH's MARS Data Analysis Software. After averaging the maximum slope after ATP stimulation of the same siRNA treatment, the effect of different siRNAs on TMEM16A function was compared with the results obtained with the non-targeting "siNEG1" siRNA treatments, using the following formula:

$$Score = \frac{Max\ slope_{siRNA} - Max\ slope_{siNEG1}}{SD_{siNEG1}}$$

Alternatively, HEK-TMEM16A-YFP were seeded at a density of 10,000 cells/well on collagen-coated 96-well plates and transfected for 48 h with plasmids or siRNAs. YFP quenching (maximum slope) was calculated as described above.

### Patch clamping

Cells grown on glass-coated cover slips were mounted on the stage of an inverted microscope (Zeiss, Munich, Germany) and kept at 37 °C. Patch pipettes were filled with a cytosolic-like solution containing (mM): KCl 30, K-gluconate 95, NaH<sub>2</sub>PO<sub>4</sub> 1.2, Na<sub>2</sub>HPO<sub>4</sub> 4.8, EGTA 1, Ca-gluconate 0.758, MgCl<sub>2</sub> 1.03, D-glucose 5, ATP 3, pH 7.2. The intracellular (pipette) Ca<sup>2+</sup> activity was 0.1 μM. Patch-clamp experiments were performed in the fast whole-cell configuration. The bath was perfused continuously with Ringer solution

containing (mM): NaCl 145, K<sub>2</sub>HPO<sub>4</sub> 1.6, MgCl<sub>2</sub> 1, KH<sub>2</sub>PO<sub>4</sub> 0.4, Ca-Gluconate 1.3, Glucose 5, pH 7.4, at a rate of 8 mL/min. TMEM16A was activated by ATP (100 μM) or ionomycin (1 μM) and CFTR was activated by IBMX (3-isobutyl-1-methylxanthine, 100 μM) and Forskolin (2 μM). Additionally, experiments were performed in the presence of 50 nM TRAM34 (Abcam, ab141885), a potent and highly selective blocker of intermediate conductance Ca<sup>2+</sup>-activated K<sup>+</sup> channels. Patch pipettes had an input resistance of 2–4 MΩ and whole cell currents were corrected for serial resistance. Currents were recorded using a patch clamp amplifier (EPC 7, List Medical Electronics, Darmstadt, Germany), the LIH1600 interface and PULSE software (HEKA, Lambrecht, Germany) as well as Chart software (AD Instruments, Spechbach, Germany). In regular intervals, membrane voltage (Vc) was clamped in steps of 20 mV from -100 to +100 mV from a holding voltage of -60 mV. Current density was calculated by dividing whole-cell currents by cell capacitance.

### Intracellular Ca<sup>2+</sup> measurements

CFBE cells were seeded on coated glass coverslips and transfected with siRNAs for 72 h. Cells were then loaded with 5 μM Fura-2/AM and 0.02% Pluronic F-127 (Life Technologies, Germany) in Ringer solution for 1 h at RT. Fluorescence was detected in cells perfused with Ringer's solution (containing (mM): NaCl 145, K<sub>2</sub>HPO<sub>4</sub> 1.6, MgCl<sub>2</sub> 1, KH<sub>2</sub>PO<sub>4</sub> 0.4, Ca-Gluconate 1.3, Glucose 5, pH 7.4) at 37 °C using an inverted microscope (Axiovert S100, Zeiss, Germany) and a highspeed polychromator system (VisiChrome, Germany). Fura-2 was excited at 340/380 nm, and emission was recorded between 470 and 550 nm using a CoolSnap camera (CoolSnap HQ, Visitron). For calibration, to obtain the maximum intracellular Ca<sup>2+</sup> concentration we added 1 μM ionomycin in Ringer. To obtain the minimum concentration of Ca<sup>2+</sup>, we used Ca<sup>2+</sup> free Ringer, where Ca-Gluconate was replaced by EGTA 5 mM. The control of the experiment, imaging acquisition and data analysis were done with the software package MetaFluor (Universal imaging, USA).

The [Ca<sup>2+</sup>]<sub>i</sub> was calculated from the 340/380 nm fluorescence ratio after background subtraction. The formula used to calculate [Ca<sup>2+</sup>]<sub>i</sub> was the following:

$$[Ca^{2+}]_i = K_d \times (R - R_{min}) / (R_{max} - R) \times (S_{f2} / S_{b2})$$

where *R* is the observed fluorescence ratio. The values *R*<sub>max</sub> and *R*<sub>min</sub> (maximum and minimum ratios) and the constant *S*<sub>f2</sub>/*S*<sub>b2</sub> (fluorescence of free and Ca<sup>2+</sup>-bound Fura-2 at 380 nm) were calculated using 1 μM ionomycin (Calbiochem), 5 μM nigericin, 10 μM monensin (Sigma-Aldrich), and 5 mM EGTA to

equilibrate intracellular and extracellular  $\text{Ca}^{2+}$  in intact Fura-2-loaded cells.

### RT-PCR

Semi-quantitative RT-PCR was performed to detect the expression of the selected genes in CFBE and HEK cells, or to quantify ADRA2C/CXCR3 knockdown. Total RNA was isolated using the NZY Total RNA Isolation kit (Nzytech, Portugal). RNA (1  $\mu\text{g}/20 \mu\text{L}$  reaction) was reverse-transcribed using random primers and NZY M-MuLV Reverse Transcriptase (Nzytech, Portugal). Each RT-PCR reaction contained sense and antisense primers for the genes of interest (0.5  $\mu\text{M}$ ) or for GAPDH (0.5  $\mu\text{M}$ ), 0.5  $\mu\text{L}$  cDNA and NZYTaq II DNA polymerase (Nzytech, Portugal). After 2 min at 95 °C cDNA was amplified during 35 cycles for 30 s at 95 °C, 30 s at 56 °C and 1 min at 72 °C. PCR products were visualized by loading on RedSafe Nucleic Acid Staining Solution (Intron Biotechnology) containing agarose gels and analysed using Image Lab (BioRad).

### Western blotting

Protein extracts were separated on 8.5% (w/v) polyacrylamide gels and transferred into polyvinylidene difluoride (PVDF) membranes. Membranes were blocked with 5% (w/v) non-fat milk powder (NFM) in Tris buffer saline with Tween 20 (TBS-T) or in PBS-T for 1 h at RT and incubated overnight at 4 °C with primary antibodies (rabbit TMEM16A antibody [Abcam, ab64085] diluted 1:500 in 1% NFM/TBS-T, mouse ADRA2C antibody [Abcam, ab167433] 1:500 in 5% PBS-T, mouse CXCR3 antibody [sc-137140 (SantaCruz)] 1:500 in 5% NFM/PBS-T, or mouse CFTR 596 antibody [Cystic Fibrosis Foundation (CFF)] 1:3000 in 5% NFM/PBS-T). Mouse  $\alpha$ -tubulin antibody diluted 1:3000 in 5% NFM/PBS-T was used as loading control. Membranes were then incubated with HRP-conjugated goat anti-rabbit/anti-mouse IgG (diluted 1:3000 in 1% or 5% NFM TBS-T or PBS-T) for 2 h at RT. Chemiluminescent detection was performed using the Clarity™ Western ECL substrate (BioRad, 170-5061) and the Chemidoc™ XRS system (BioRad). The quantification of band intensity was performed using the Image Lab software (BioRad) and normalized to the loading control as appropriate.

### cAMP measurements

HEK cells were transfected with a fluorescence resonance energy transfer (FRET)-based Epac cAMP sensor (YFP-Epac-CFP)<sup>38,39</sup> to analyse changes in intracellular cAMP levels. When expressed in cells, YFP-Epac-CFP displays significant FRET, due to close proximity of CFP (donor) and YFP (acceptor). Rises in cAMP levels induce

a conformational change that rapidly lowers FRET, which can then be recovered by adding cAMP-lowering agents.<sup>67</sup> Therefore, increases in the ratio CFP/YFP (measured using a fluorescence microscope) indicate higher concentrations of cAMP and, consequently, unfolding of Epac. Differences in cAMP levels in HEK cells transfected with either ADRA2C or CXCR3 were measured using the ratio CFP fluorescence/YFP fluorescence.  $G_i$  protein-coupled signalling pathways were inhibited by pertussis toxin (PTX), increasing intracellular cAMP, thus augmenting the FRET signal. Adenylyl cyclase (AC) stimulation by forskolin and phosphodiesterase inhibition with IBMX were also used to increase cAMP levels.

### Statistical analyses

Data are reported as means  $\pm$  SEM. Two-tailed student's *t*-test (for paired or unpaired samples as appropriate) or ANOVA were used for statistical analysis. A value of  $p < 0.05$  was accepted as a significant difference. The number of experiments performed (*n*) is indicated in figure legends.

### CRedit authorship contribution statement

**Madalena C. Pinto:** Conceptualization, Methodology, Writing – original draft, Writing – review & editing, Formal analysis. **Hugo M. Botelho:** Formal analysis, Writing – review & editing, Conceptualization, Methodology, Software. **Iris A.L. Silva:** Writing – review & editing. **Violeta Railean:** Writing – review & editing. **Beate Neumann:** Conceptualization, Writing – review & editing. **Rainer Pepperkok:** Conceptualization, Writing – review & editing. **Rainer Schreiber:** Formal analysis, Writing – review & editing. **Karl Kunzelmann:** Writing – review & editing, Conceptualization, Funding acquisition. **Margarida D. Amaral:** Writing – original draft, Writing – review & editing, Conceptualization, Methodology, Funding acquisition.

### Acknowledgements

Work supported by UIDB/04046/2020 and UIDP/04046/2020 centre grants from FCT/MCTES Portugal (to BioISI) and research grant (to MDA), and SRC 013 from CF Trust/ UK. MCP was recipient of SFRH/PD/BD/114393/2016 fellowship from BioSys PhD programme PD/00065/2012 from FCT (Portugal).

Part of imaging and analysis done at the Faculty of Sciences of the University of Lisbon's Microscopy Facility, a node of the Portuguese

Platform for BioImaging, reference PPBI-POCI-01-0145-FEDER-022122.

The authors are also grateful to Luís Marques (BioISI), to staff from EMBL, Heidelberg (Germany), namely from ALMF-Advanced Light Microscopy (Christian Tischer, Sabine Reither) and Flow Cytometry (Malte Paulsen) core facilities, and to Dr. Vladimir M. Milenkovic (University of Regensburg) for technical assistance.

## Declaration of Competing Interest

The authors declare that they have no known competing financial interests or personal relationships that could have appeared to influence the work reported in this paper.

## Appendix A. Supplementary material

Supplementary data to this article can be found online at <https://doi.org/10.1016/j.jmb.2021.167436>.

Received 22 October 2021;  
Accepted 28 December 2021;  
Available online 3 January 2022

### Keywords:

secretory traffic;  
TMEM16A;  
Ca<sup>2+</sup>-activated Cl<sup>-</sup> channels;  
cystic fibrosis;  
G-protein coupled receptors

### Abbreviations:

ANO/TMEM16, Anoctamin; CaCC, calcium (Ca<sup>2+</sup>)-activated chloride (Cl<sup>-</sup>) channel; CF, cystic fibrosis; CFBE, cystic fibrosis bronchial epithelial (cells); CFTR, cystic fibrosis transmembrane conductance regulator; Dox, doxycycline; ER, endoplasmic reticulum; GPCR, G-protein coupled receptor; HA, hemagglutinin; HTS, high-throughput screening; PM, plasma membrane; WB, Western blot

## References

- Riordan, J.R., Rommens, J.M., Kerem, B., Alon, N.O.A., Rozmahel, R., Grzelczak, Z., Zielenski, J., Lok, S., et al., (1989). Identification the cystic fibrosis gene: Cloning and characterization of complementary DNA. *Science (80-)* **245**, 1066–1073.
- O'Sullivan, B.P., Freedman, S.D., (2009). Cystic fibrosis. *Lancet* **373**, 1891–1904. [https://doi.org/10.1016/S0140-6736\(09\)60327-5](https://doi.org/10.1016/S0140-6736(09)60327-5).
- Hug, M.J., Tamada, T., Bridges, R.J., (2003). CFTR and bicarbonate secretion by epithelial cells. *News Physiol. Sci.* **18**, 38–42.
- Verkman, A.S., Song, Y., Thiagarajah, J.R., (2003). Role of airway surface liquid and submucosal glands in cystic fibrosis lung disease. *Am. J. Physiol. Cell Physiol.* **284**, C2–C15. <https://doi.org/10.1152/ajpcell.00417.2002>.
- Turcios, N.L., (2020). Cystic fibrosis lung disease: An overview. *Respir. Care* **65**, 233–251. <https://doi.org/10.4187/respcare.06697>.
- Heijerman, H.G.M., McKone, E.F., Downey, D.G., Van Braeckel, E., Rowe, S.M., Tullis, E., Mall, M.A., Welter, J.J., et al., (2019). Efficacy and safety of the elexacaftor plus tezacaftor plus ivacaftor combination regimen in people with cystic fibrosis homozygous for the F508del mutation: a double-blind, randomised, phase 3 trial. *Lancet* **394**, 1940–1948. [https://doi.org/10.1016/S0140-6736\(19\)32597-8](https://doi.org/10.1016/S0140-6736(19)32597-8).
- Middleton, P.G., Mall, M.A., Dřevínek, P., Lands, L.C., McKone, E.F., Polineni, D., Ramsey, B.W., Taylor-Cousar, J.L., et al., (2019). Elexacaftor-tezacaftor-ivacaftor for cystic fibrosis with a single Phe508del allele. *N. Engl. J. Med.* **381**, 1809–1819. <https://doi.org/10.1056/NEJMoa1908639>.
- De Boeck, K., Amaral, M.D., (2016). Progress in therapies for cystic fibrosis. *Lancet Respir. Med.* **4**, 662–674. [https://doi.org/10.1016/S2213-2600\(16\)00023-0](https://doi.org/10.1016/S2213-2600(16)00023-0).
- ECFS Patient Registry Annual Data Report 2018, 2018.
- Pranke, I., Golec, A., Hinzpeter, A., Edelman, A., Sermet-Gaudelus, I., (2019). Emerging therapeutic approaches for cystic fibrosis. From gene editing to personalized medicine. *Front. Pharmacol.* **10**, 1–21. <https://doi.org/10.3389/fphar.2019.00121>.
- Yang, Y.D., Cho, H., Koo, J.Y., Tak, M.H., Cho, Y., Shim, W.-S., Park, S.P., Lee, J., et al., (2008). TMEM16A confers receptor-activated calcium-dependent chloride conductance. *Nature* **455**, 1210–1215. <https://doi.org/10.1038/nature07313>.
- Caputo, A., Caci, E., Ferrera, L., Pedemonte, N., Barsanti, C., Sondo, E., Pfeiffer, U., Ravazzolo, R., et al., (2008). TMEM16A, a membrane protein associated with calcium-dependent chloride channel activity. *Science* **322**, 590–594. <https://doi.org/10.1126/science.1163518>.
- Schroeder, B.C., Cheng, T., Jan, Y.N., Jan, L.Y., (2008). Expression cloning of TMEM16A as a calcium-activated chloride channel subunit. *Cell* **134**, 1019–1029. <http://www.sciencedirect.com/science/article/B6WSN-4TG9M0B-M/2/e966b6f40899852dfb45d74ee9dbd60d>.
- Milenkovic, V.M., Brockmann, M., Stöhr, H., Weber, B.H., Strauss, O., (2010). Evolution and functional divergence of the anoctamin family of membrane proteins. *BMC Evol. Biol.* **10**, 319. <https://doi.org/10.1186/1471-2148-10-319>.
- Sondo, E., Caci, E., Galletta, L.J.V., (2014). The TMEM16A chloride channel as an alternative therapeutic target in cystic fibrosis. *Int. J. Biochem. Cell Biol.* **52**, 73–76. <https://doi.org/10.1016/j.biocel.2014.03.022>.
- Gentzsch, M., Mall, M.A., (2018). Ion channel modulators in cystic fibrosis. *Chest* **154**, 383–393. <https://doi.org/10.1016/j.chest.2018.04.036>.
- Mall, M.A., Mayer-Hamblett, N., Rowe, S.M., (2020). Cystic fibrosis: Emergence of highly effective targeted therapeutics and potential clinical implications. *Am. J. Respir. Crit. Care Med.* **201**, 1193–1208. <https://doi.org/10.1164/rccm.201910-1943SO>.
- Ousingsawat, J., Martins, J.R., Schreiber, R., Rock, J.R., Harfe, B.D., Kunzelmann, K., (2009). Loss of TMEM16A causes a defect in epithelial Ca<sup>2+</sup>-dependent chloride transport. *J. Biol. Chem.* **284**, 28698–28703. <https://doi.org/10.1074/jbc.M109.012120>.
- Rock, J.R., O'Neal, W.K., Gabriel, S.E., Randell, S.H., Harfe, B.D., Boucher, R.C., Grubb, B.R., (2009). Transmembrane protein 16A (TMEM16A) is a Ca<sup>2+</sup>-

- regulated Cl<sup>-</sup> secretory channel in mouse airways. *J. Biol. Chem.* **284**, 14875–14880. <https://doi.org/10.1074/jbc.C109.000869>.
20. Romanenko, V.G., Catalán, M.A., Brown, D.A., Putzier, I., Hartzell, H.C., Marmorstein, A.D., Gonzalez-Begne, M., Rock, J.R., et al., (2010). Tmem16A encodes the Ca<sup>2+</sup>-activated Cl<sup>-</sup> channel in mouse submandibular salivary gland acinar cells. *J. Biol. Chem.* **285**, 12990–13001. <https://doi.org/10.1074/jbc.M109.068544>.
21. Lin, J., Jiang, Y., Li, L., Liu, Y., Tang, H., Jiang, D., (2015). TMEM16A mediates the hypersecretion of mucus induced by Interleukin-13. *Exp. Cell Res.* **334**, 260–269. <https://doi.org/10.1016/j.yexcr.2015.02.026>.
22. Benedetto, R., Cabrita, I., Schreiber, R., Kunzelmann, K., (2019). TMEM16A is indispensable for basal mucus secretion in airways and intestine. *FASEB J.* **33**, 4502–4512. <https://doi.org/10.1096/fj.201801333RRR>.
23. Kunzelmann, K., Ousingasawat, J., Cabrita, I., Doušová, T., Bähr, A., Janda, M., Schreiber, R., Benedetto, R., (2019). TMEM16A in cystic fibrosis: Activating or inhibiting? *Front. Pharmacol.* **9**, 1–18. <https://doi.org/10.3389/fphar.2019.00003>.
24. Huang, F., Zhang, H., Wu, M., Yang, H., Kudo, M., Peters, C.J., Woodruff, P.G., Solberg, O.D., et al., (2012). Calcium-activated chloride channel TMEM16A modulates mucin secretion and airway smooth muscle contraction. *Proc. Natl. Acad. Sci. U. S. A.* **109**, 16354–16359. <https://doi.org/10.1073/pnas.1214596109>.
25. Simões, F.B., Quaresma, M.C., Clarke, L.A., Silva, I.A.L., Pankonien, I., Railean, V., Kmit, A., Amaral, M.D., (2019). TMEM16A chloride channel does not drive mucus production. *Life Sci. Alliance* **2**, 1–13. <https://doi.org/10.26508/LSA.201900462>.
26. Danahay, H.L., Lilley, S., Fox, R., Charlton, H., Sabater, J., Button, B., McCarthy, C., Collingwood, S.P., et al., (2020). TMEM16A Potentiation: A Novel Therapeutic Approach for the Treatment of Cystic Fibrosis. *Am. J. Respir. Crit. Care Med.* **201**, 946–954. <https://doi.org/10.1164/rccm.201908-1641OC>.
27. Danahay, H., Fox, R., Lilley, S., Charlton, H., Adley, K., Christie, L., Ansari, E., Ehre, C., et al., (2020). Potentiating TMEM16A does not stimulate airway mucus secretion or bronchial and pulmonary arterial smooth muscle contraction. *FASEB BioAdv.* **2**, 464–477. <https://doi.org/10.1096/fba.2020-00035>.
28. Benedetto, R., Ousingasawat, J., Wanitchakool, P., Zhang, Y., Holtzman, M.J., Amaral, M., Rock, J.R., Schreiber, R., et al., (2017). Epithelial Chloride Transport by CFTR Requires TMEM16A. *Sci. Rep.* **7**, 1–13. <https://doi.org/10.1038/s41598-017-10910-0>.
29. Lérias, J.R., Pinto, M.C., Botelho, H.M., Awatade, N.T., Quaresma, M.C., Silva, I.A.L., Wanitchakool, P., Schreiber, R., et al., (2018). A novel microscopy-based assay identifies extended synaptotagmin-1 (ESYT1) as a positive regulator of anoctamin 1 traffic. *Biochim. Biophys. Acta – Mol. Cell Res.* **1865**, 421–431. <https://doi.org/10.1016/j.bbamcr.2017.11.009>.
30. Lérias, J., Pinto, M., Benedetto, R., Schreiber, R., Amaral, M., Aureli, M., Kunzelmann, K., (2018). Compartmentalized crosstalk of CFTR and TMEM16A (ANO1) through EPAC1 and ADCY1. *Cell. Signal.* **44**, 10–19. <https://doi.org/10.1016/j.cellsig.2018.01.008>.
31. Botelho, H.M., Uliyakina, I., Awatade, N.T., Proença, M.C., Tischer, C., Sirianant, L., Kunzelmann, K., Pepperkok, R., et al., (2015). Protein traffic disorders: An effective high-throughput fluorescence microscopy pipeline for drug discovery. *Sci. Rep.* **5**, 1–8. <https://doi.org/10.1038/srep09038>.
32. Ashburner, M., Ball, C.A., Blake, J.A., Botstein, D., Butler, H., Cherry, J.M., Davis, A.P., Dolinski, K., et al., (2000). Gene Ontology: tool for the unification of biology. *Nature Genet.* **25**, 25–29.
33. Carbon, S., Douglass, E., Dunn, N., Good, B., Harris, N.L., Lewis, S.E., Mungall, C.J., Basu, S., et al., (2019). The Gene Ontology Resource: 20 years and still GOing strong. *Nucleic Acids Res.* **47**, D330–D338. <https://doi.org/10.1093/nar/gky1055>.
34. Schreiber, Rainer, Uliyakina, Inna, Kongsuphol, Patthara, Warth, Richard, Mirza, Myriam, Martins, Joana R., Kunzelmann, K., (2010). Expression and function of epithelial anoctamins. *Journal of Biological Chemistry.* <https://doi.org/10.1074/jbc.M109.065367>.
35. Calzada, Beatriz C., De Artiñano, Amaya A., (2001). Alpha-adrenoceptor subtypes. *Pharmacological Research* **44** <https://doi.org/10.1006/phrs.2001.0857>.
36. Rossi, Devora, Zlotnik, Albert, (2000). The Biology of Chemokines and Their Receptors. *Annu. Rev. Immunol.* **18** <https://doi.org/10.1146/annurev.immunol.18.1.217>.
37. Hepler, John R., Gilman, Alfred G., (1992). G-proteins. *Trends in Biochemical Sciences.* [https://doi.org/10.1016/0968-0004\(92\)90005-T](https://doi.org/10.1016/0968-0004(92)90005-T).
38. Klarenbeek, J., Goedhart, J., Van Batenburg, A., Groenewald, D., Jalink, K., (2015). Fourth-generation Epac-based FRET sensors for cAMP feature exceptional brightness, photostability and dynamic range: Characterization of dedicated sensors for FLIM, for ratiometry and with high affinity. *PLoS One* **10**, 1–11. <https://doi.org/10.1371/journal.pone.0122513>.
39. Storch, U., Straub, J., Erdogmus, S., Gudermann, T., Mederos y Schnitzler, M., (2017). Dynamic monitoring of Gi/o-protein-mediated decreases of intracellular cAMP by FRET-based Epac sensors. *Pflugers Arch. Eur. J. Physiol.* **469**, 725–737. <https://doi.org/10.1007/s00424-017-1975-1>.
40. Carbonetti, N.H., (2010). Pertussis toxin and adenylate cyclase toxin: key virulence factors of Bordetella pertussis and cell biology tools. *Futur. Microbiol.* **455–469** <https://doi.org/10.2217/fmb.09.133>.
41. Lee, Y.S., Bae, Y., Park, N., Yoo, J.C., Cho, C.H., Ryoo, K., Hwang, E.M., Park, J.Y., (2016). Surface expression of the Anoctamin-1 (ANO1) channel is suppressed by protein-protein interactions with β-COP. *Biochem. Biophys. Res. Commun.* **475**, 216–222. <https://doi.org/10.1016/j.bbrc.2016.05.077>.
42. Boucrot, E., Saffarian, S., Zhang, R., Kirchhausen, T., (2010). Roles of AP-2 in clathrin-mediated endocytosis. *PLoS One* **5** <https://doi.org/10.1371/journal.pone.0010597>.
43. Pinto, M.C., Schreiber, R., Lérias, J.R., Ousingasawat, J., Duarte, A., Amaral, M.D., Kunzelmann, K., (2020). Regulation of TMEM16A by CK2 and Its Role in Cellular Proliferation. *Cells* **9** <https://doi.org/10.3390/cells9051138>.
44. West, R.B., Corless, C.L., Chen, X., Rubin, B.P., Subramanian, S., Montgomery, K., Zhu, S., Ball, C.A., et al., (2004). The novel marker, DOG1, is expressed ubiquitously in gastrointestinal stromal tumors irrespective of KIT or PDGFRA mutation status. *Am. J. Pathol.* **165**, 107–113. [https://doi.org/10.1016/S0002-9440\(10\)63279-8](https://doi.org/10.1016/S0002-9440(10)63279-8).
45. Carles, A., Millon, R., Cromer, A., Ganguli, G., Lemaire, F., Young, J., Wasylyk, C., Muller, D., et al., (2006). Head and

- neck squamous cell carcinoma transcriptome analysis by comprehensive validated differential display. *Oncogene* **25**, 1821–1831. <https://doi.org/10.1038/sj.onc.1209203>.
46. Britschgi, A., Bill, A., Brinkhaus, H., Rothwell, C., Clay, I., Duss, S., Rebhan, M., Raman, P., et al., (2013). Calcium-activated chloride channel ANO1 promotes breast cancer progression by activating EGFR and CAMK signaling. *Proc. Natl. Acad. Sci. U. S. A.* **110** <https://doi.org/10.1073/pnas.1217072110>.
47. Jia, L., Liu, W., Guan, L., Lu, M., Wang, K.W., (2015). Inhibition of calcium-activated chloride channel ANO1/TMEM16A suppresses tumor growth and invasion in human lung cancer. *PLoS One* **10**, 1–17. <https://doi.org/10.1371/journal.pone.0136584>.
48. Duvvuri, U., Shiwarshi, D.J., Xiao, D., Bertrand, C., Huang, X., Edinger, R.S., Rock, J.R., Harfe, B.D., et al., (2012). TMEM16A induces MAPK and contributes directly to tumorigenesis and cancer progression. *Cancer Res.* **72**, 3270–3281. <https://doi.org/10.1158/0008-5472.CAN-12-0475-T>.
49. Ruiz, C., Martins, J.R., Rudin, F., Schneider, S., Dietsche, T., Fischer, C.A., Tornillo, L., Terracciano, L.M., et al., (2012). Enhanced expression of ANO1 in head and neck squamous cell carcinoma causes cell migration and correlates with poor prognosis. *PLoS One* **7** <https://doi.org/10.1371/journal.pone.0043265>.
50. Benedetto, R., Ousingsawat, J., Cabrita, I., Pinto, M., Lérias, J.R., Wanitchakool, P., Schreiber, R., Kunzelmann, K., (2019). Plasma membrane-localized TMEM16 proteins are indispensable for expression of CFTR. *J. Mol. Med.* <https://doi.org/10.1007/s00109-019-01770-4>.
51. Almaça, J., Faria, D., Sousa, M., Uliyakina, I., Conrad, C., Sirianant, L., Clarke, L.A., Martins, J.P., et al., (2013). High-content siRNA screen reveals global ENaC regulators and potential cystic fibrosis therapy targets. *Cell* **154**, 1390. <https://doi.org/10.1016/j.cell.2013.08.045>.
52. Simpson, J.C., Joggerst, B., Laketa, V., Verissimo, F., Cetin, C., Erfle, H., Bexiga, M.G., Singan, V.R., et al., (2012). Genome-wide RNAi screening identifies human proteins with a regulatory function in the early secretory pathway. *Nature Cell Biol.* **14**, 764–774. <https://doi.org/10.1038/ncb2510>.
53. Neumann, B., Walter, T., Hériché, J.K., Bulkescher, J., Erfle, H., Conrad, C., Rogers, P., Poser, I., et al., (2010). Phenotypic profiling of the human genome by time-lapse microscopy reveals cell division genes. *Nature* **464**, 721–727. <https://doi.org/10.1038/nature08869>.
54. Dibner, M.D., Insel, P.A., (1981). Serum catecholamines desensitize  $\beta$ -adrenergic receptors of cultured C6 glioma cells. *J. Biol. Chem.* **256**, 7343–7346. [https://doi.org/10.1016/s0021-9258\(19\)68968-4](https://doi.org/10.1016/s0021-9258(19)68968-4).
55. Dorn, G.W., Oswald, K.J., McCluskey, T.S., Kuhel, D.G., Liggett, S.B., (1997).  $\alpha(2A)$ -Adrenergic receptor stimulated calcium release is transduced by G(i)-associated G( $\beta\gamma$ )-mediated activation of phospholipase C. *Biochemistry* **36**, 6415–6423. <https://doi.org/10.1021/bi970080s>.
56. Smit, M.J., Verdijk, P., Van der Raaij-Helmer, E.M.H., Navis, M., Hensbergen, P.J., Leurs, R., Tensen, C.P., (2003). CXCR3-mediated chemotaxis of human T cells is regulated by a G i-and phospholipase C-dependent pathway and not via activation of MEK/p44/p42 MAPK nor Akt/PI-3 kinase. *Blood* **102**, 1959–1965. <https://doi.org/10.1182/blood-2002-12-3945>.
57. Cuiñas, A., García-Morales, V., Viña, D., Gil-Longo, J., Campos-Toimil, M., (2016). Activation of PKA and Epac proteins by cyclic AMP depletes intracellular calcium stores and reduces calcium availability for vasoconstriction. *Life Sci.* **155**, 102–109. <https://doi.org/10.1016/j.lfs.2016.03.059>.
58. Ferguson, S.S.G., Downey, W.E., Colapietro, A.M., Barak, L.S., Ménard, L., Caron, M.G., (1996). Role of  $\beta$ -arrestin in mediating agonist-promoted G protein-coupled receptor internalization. *Science (80-.)* **271**, 363–366. <https://doi.org/10.1126/science.271.5247.363>.
59. Zhang, J., Barak, L.S., Winkler, K.E., Caron, M.G., Ferguson, S.S.G., (1997). A central role for  $\beta$ -arrestins and clathrin-coated vesicle-mediated endocytosis in  $\beta$ 2-adrenergic receptor resensitization. Differential regulation of receptor resensitization in two distinct cell types. *J. Biol. Chem.* **272**, 27005–27014. <https://doi.org/10.1074/jbc.272.43.27005>.
60. Olli-Lähdesmäki, T., Scheinin, M., Pohjanoksa, K., Kallio, J., (2003). Agonist-dependent trafficking of  $\alpha$ 2-adrenoceptor subtypes: Dependence on receptor subtype and employed agonist. *Eur. J. Cell Biol.* **82**, 231–239. <https://doi.org/10.1078/0171-9335-00311>.
61. Meiser, A., Mueller, A., Wise, E.L., McDonagh, E.M., Petit, S.J., Saran, N., Clark, P.C., Williams, T.J., et al., (2008). The Chemokine Receptor CXCR3 Is Degraded following Internalization and Is Replenished at the Cell Surface by De Novo Synthesis of Receptor. *J. Immunol.* **180**, 6713–6724. <https://doi.org/10.4049/jimmunol.180.10.6713>.
62. Ameen, N., Silvis, M., Bradbury, N.A., (2007). Endocytic trafficking of CFTR in health and disease. *J. Cyst. Fibros* **6**, 1–14. <https://www.ncbi.nlm.nih.gov/pmc/articles/PMC3624763/pdf/nihms412728.pdf>.
63. Pley, U., Parham, P., Brodsky, F.M., (1993). Clathrin: Its role in receptor-mediated vesicular transport and specialized functions in neurons. *Crit. Rev. Biochem. Mol. Biol.* **28**, 431–464. <https://doi.org/10.3109/10409239309078441>.
64. Lau, A.W., Chou, M.M., (2008). The adaptor complex AP-2 regulates post-endocytic trafficking through the non-clathrin Arf6-dependent endocytic pathway. *J. Cell Sci.* **121**, 4008–4017. <https://doi.org/10.1242/jcs.033522>.
65. Erfle, H., Neumann, B., Rogers, P., Bulkescher, J., Ellenberg, J., Pepperkok, R., (2008). Work flow for multiplexing siRNA assays by solid-phase reverse transfection in multiwell plates. *J. Biomol. Screen.* **13**, 575–580. <https://doi.org/10.1177/1087057108320133>.
66. Galletta, L.J.V., Haggie, P.M., Verkman, A.S., (2001). Green fluorescent protein-based halide indicators with improved chloride and iodide affinities. *FEBS Lett.* **499**, 220–224. [https://doi.org/10.1016/S0014-5793\(01\)02561-3](https://doi.org/10.1016/S0014-5793(01)02561-3).
67. Ponsoen, B., Zhao, J., Riedl, J., Zwartkruis, F., van der Krogt, G., Zaccolo, M., Moolenaar, W.H., Bos, J.L., et al., (2004). Detecting cAMP-induced Epac activation by fluorescence resonance energy transfer: Epac as a novel cAMP indicator. *EMBO Rep.* **5**, 1176–1180. <https://doi.org/10.1038/sj.embor.7400290>.